





Geomorphic assessment of active tectonics in Jaisalmer basin (Western Rajasthan, India)

Mery Biswas, Manash Pratim Gogoi, Bikramaditya Mondal, Thota Sivasankar, Soumyajit Mukherjee & Swagato Dasgupta


To cite this article: Mery Biswas, Manash Pratim Gogoi, Bikramaditya Mondal, Thota Sivasankar, Soumyajit Mukherjee & Swagato Dasgupta (2022) Geomorphic assessment of active tectonics in Jaisalmer basin (Western Rajasthan, India), Geocarto International, 37:26, 12382-12413, DOI: [10.1080/10106049.2022.2066726](https://doi.org/10.1080/10106049.2022.2066726)

To link to this article: <https://doi.org/10.1080/10106049.2022.2066726>

 View supplementary material [↗](#)


 Published online: 20 May 2022.

 Submit your article to this journal [↗](#)

 Article views: 356

 View related articles [↗](#)

 View Crossmark data [↗](#)

 Citing articles: 5 View citing articles [↗](#)



Geomorphic assessment of active tectonics in Jaisalmer basin (Western Rajasthan, India)

Mery Biswas^a, Manash Pratim Gogoi^b, Bikramaditya Mondal^c,
Thota Sivasankar^d , Soumyajit Mukherjee^c and Swagato Dasgupta^e

^aDepartment of Geography, Presidency University, Kolkata, West Bengal, India; ^bDepartment of Geology, Sibsagar College, Joysagar, Assam, Sivasagar, India; ^cDepartment of Earth Sciences, Indian Institute of Technology Bombay, Powai, Maharashtra, Mumbai, India; ^dNIIT University, Neemrana, Rajasthan, India; ^eDepartment of Applied Geophysics, Indian Institute of Technology (ISM), Dhanbad, Jharkhand, India

ABSTRACT

The northwestern part of Indian plate consists of a number of sedimentary basins such as the Jaisalmer basin with Early Jurassic to Quaternary deposits. The NW-SE trending Kanoi fault and Ramgarh fault with Mari-Jaisalmer Arch in the basin are tectonically active. We delineate the tectonically active areas of the basin by considering watersheds, micro-scale basins and spot locations. Analytic Hierarchy Process (AHP) is applied to calculate the Index of Active Tectonics (IAT) for the watersheds. Basin asymmetry (AF), valley floor width to height ratio (Vf) and hypsometric curve are calculated/generated. Computed R2 values and the IAT identify watershed-4, Miajlai depression, to be tectonically most active. Three individual spots along the NW-trending Mari highland have tectonic control on drainage patterns. The hydrocarbon fields are located in the Shahgarh and the Miajlar depression zones within watersheds 3 and 4, which are under tectonically moderate and high activities, respectively.

ARTICLE HISTORY

Received 13 October 2021
Accepted 10 April 2022

KEYWORDS

Tectonic geomorphology;
petroleum geoscience;
structural geology;
active tectonics


HIGHLIGHTS

- I. Geomorphology of the Jaisalmer basin in response to active tectonics is investigated.
- II. Watershed 4 is tectonically active followed by watershed 3. Hydrocarbon fields are located in these two watersheds.
- III. The work will have far-reaching implication in petroleum geosciences of the area.

1. Introduction

Hydrocarbon-bearing sedimentary basins possess enormous international attention for exploration purpose (e.g. Dasgupta and Mukherjee 2017; Dasgupta and Mukherjee 2019; Dasgupta et al. 2022). Field-specific geoscientific investigations to identify (new) locations for hydrocarbon exploration becomes more challenging when rock outcrops are scarce

CONTACT Soumyajit Mukherjee  soumyajitm@gmail.com, smukherjee@iitb.ac.in

 Supplemental data for this article can be accessed online at <https://doi.org/10.1080/10106049.2022.2066726>

and are mostly covered by surficial deposits. Jaisalmer basin is one such enigmatic example from the western Rajasthan, India (e.g. Nigam et al. 1989; Pandey et al. 2019a, 2019b; Pandey and Maurya 2020). Despite several paleontologic and lithologic studies conducted in this basin leading to a fairly well known stratigraphy (Table 1), its (morpho)tectonic (field-based structural) data have been scanty.

Tectonically, there are three main provinces in Jaisalmer basin: (i) raised Mari–Jaisalmer high, (ii) synclinal Shahgarh, and (iii) monoclinical Kishangarh and Miajlar shelf. Shallow marine deposits dominantly exist in the Jaisalmer basin. The Bhadasar Formations deposited in the Middle to Late Jurassic Period. Uplift initiated during the Upper Cretaceous to the Lower Paleocene and incision exposed the Cretaceous sequences following the axial high up to the basin margin area.

The Jaisalmer basin experienced several tectonic events along with distinct brittle deformations- faulting and fracturing. The geo-tectonic set up has refined the morphologic layout with arid cycles of uplift/incision sequence, which established the pediments over the flat terrain, inselberg (eroded hills) and playas. Application of geomorphic indicators with respect to the linear and watersheds/basin to constrain the Index of Active Tectonics (IAT) of the Jaisalmer shelf area had remained a due.

In this study, we have considered only the Jaisalmer shelf within the Indian territory for morphometric analysis. The Indus shelf part in Pakistan is not considered.

Tectonic activities strongly control the morphology or any faulting within the sedimentary basin. The spatial indicators viz., Basin Shape Index (Bs), Transverse Topographic Symmetry Factor (T), Hypsometric Integral (HI), Elongation Ratio (Re), Circularity Ratio (Rc), Tilt angle (β) and Form Factor (Rf) are related with slope. Linear morphometric parameters such as SL and SI also connote tectonic activity; e.g. uplift-induced steep valley-cutting and straight nature of channel flow path. Presence of major fault lines lead to the higher SL values. River basin displaced due to tectonic activity is rather rare. More common are channel shift, increased headword erosion and river piracy.

This work performs morphotectonic analyses of the Jaisalmer basin. This is achieved in three steps: (i) analyses of lineaments from Google Earth images; (ii) delineation of basins/watersheds from DEM with the detail application of relief-scale/watershed or basin scale aspects and drainage patterns; and (iii) evaluation of linear-scale parameters and basin/watershed-scale indicators to specify the Index of Active Tectonics.

We identify tectonically active watershed areas in the Jaisalmer basin and point out that sub-surface fault reactivation has happened near the Kanoi fault, Manhera fault and Manhera Tibba structure.

2. Geology

The Jaisalmer basin is a shelf-zone of the Indus geosyncline, which is separated from the Bikaner-Nagaur basin by the Pokhran-Nachna high in the northwest and Barmer basin by the Banner-Birmama-Nagarparkar high/Fatehgarh fault in the south. The Jaisalmer basin is marked as a NW-SE trending regional fault-bound zone from Jaisalmer up to around Mari (Awasthi 2002).

Sedimentary cycle started in Permian Period with the deposits of shales and sandstones of Karampur Formation, which is overlain by Triassic Sumarwali Formation, Jaisalmer Lathi of Middle to Lower Jurassic (Bonde 2010). Baisakhi, and Bhadasar Formation deposited in Middle to Late Jurassic Periods. Cretaceous deposits known as Pariwar Formation overlie the Jurassic sediments. This is followed by Parh in Upper Cretaceous, Sanu in Paleocene, Khuila in lower Eocene, Bandah in middle Eocene and lastly Sumar in Pleistocene to recent (Pandey et al. 2006; Patra and Sukla 2020); (Table 1).

Table 1. Stratigraphy of Jaisalmer Basin compiled from publications.

Age/Series/Formation	Lithology/key features
Recent	
Windblown sand/alluvium ^{a,d,e,v}	Loose sand and alluvial material
Dune sand, Alluvium Gravel/Trap wash ¹¹	
Recent – Pleistocene	
Shumar ^{a,c,d,e,g,o,q,t,v,w,x,y,z,1,2,3,5,7,8,12,13.}	Dune sand, gravel with ferruginous nodules, limestone. Mainly gravels with ferruginous nodules cemented, at places limestone cobbles forming pseudo conglomerate, occasionally coarse grained ferruginous sandstones, eolian sand with streaks of argillaceous, calcareous sandstone, intercalated limestone and variegated clay.
α-Member ^q	Loose sand
β-Member ^q	Limestone and Calc. sandstone
γ-Member ^q	Sandstone and variegated clays
δ-Member ^q	Alternating variegated clays, sandstone and glauconitic clay
Uttarlai ¹¹	
Middle Eocene	
Bundah ^{a,c,d,e,g,o,q,u,v,w,x,y,z,1,2,3,5,7,8,11,12,13}	Foraminiferal limestone, clays at base, glauconitic clay, alternations of grey shale and grey to greenish grey argillaceous, foraminiferal limestone
(Kirthar) ^{q,u,3}	
Bakhri Tibba ^{q,8}	Clay, limestone
Habib Rahi ^q	Clay, limestone
Bandah ^t	
Bakhri Tibba Limestone ^{t,5}	Glauconitic calcareous sand, Greyish white hard foraminiferal limestone
Batrewala Limestone ^{t,5,7,8}	Alternations of grey shale and greenish grey, argillaceous Foraminiferal limestone. Greyish white to pinkish white hard, compact, foraminiferal limestone becoming argillaceous at base.
Kinsar shale member ⁵	Gypseous, orcherous, yellow shales with whitish yellow, argillaceous, thin limestone beds, calcareous silts and foraminiferal test beds.
Lower Eocene	
Khuiala ^{a,c,d,e,g,v,w,x,y,z,1,2,3,5,11,13}	Shales with limestone beds and calcareous silts.
Lower Eocene – Paleocene	
Khuiala ^{q,u,12,13}	
(Laki) ^{q,r,u}	Shale, Limestone
Up. Ghazij ^q	Shale
Lr. Ghazij ^q	Limestone, marl
Dunghan ^q	
Khuiala ^{t,8}	Greenish grey, micaceous fissile shale with intercalated limestone, bioclastics with interbeds of shale
Upper Khinsar Shale ^{t,7,8}	
Sirhera ^{t,7,8}	
Lower Khinsar Shale ^{t,7,8}	
Tetakkar ^{t,5,7,8}	Bioclastic limestone with inter beds of shale Creamish white to buff, hard compact, microcrystalline limestone in up[per part and alternations of yellow shales and argillaceous limestone/ calcareous claystone in the lower part.
Palaeocene	
Sanu ^{a,c,d,e,g,o,q,t,v,w,x,y,z,1,2,3,5,7,8,11,12,13}	Friable sandstone with minor clays, marl, limestone, shale, silty clay, sandstone with lignite, sandstone with coquina bed and glauconite.
(Ranikot) ^{q,r,u}	
Kharatar ^{t,8}	Alternations of sand, marl and argillaceous limestone and glauconitic sand at base
Mohamad dhani ^{t,5,7,8}	Sandstone, medium to coarse, friable, at places, glauconitic with shale. Quartzose yellow to maroon, ferruginous, friable cross bedded sandstone with minor purplish white clays, ferruginous at base, siltstone, dark grey carbonaceous shale.
Upper Cretaceous	
Turonian -Coniacian	
Parh ^{a,c,d,e,g,q,u,w,x,z,1,2,3,8,11,12,13}	Marls, arenaceous limestone, argillaceous limestone, clay and marl, interbeds of grey to greenish grey limestone, greenish grey silty, feebly calcareous shale

(continued)

Table 1. Continued.

Age/Series/Formation	Lithology/key features
Aptian – Turonian Goru ^{a,c,d,e,f,g,q,u,w,11,12,13}	Sandstone and shale. Shale with glauconites, clay, Marl, shale, clay, calcareous siltstone and shale Sandstone, shale, calcareous siltstone, argillaceous sandstone, glauconitic very fine sandstone and silty, sideritic claystone Glauconitic towards base.
Up. Goru ^{q,x,z,1,2,3} Lr. Goru ^{q,x,z,1,2,3,7}	
Cenomanian	Mainly greenish grey to grey feebly calcareous pyritic shale at places silty marls beds towards top
Up. Goru ⁸	
Albian –Aptian Lr. Goru ⁸	Alternations of light grey fine grained glauconitic sandstone and grey shale, towards bottom shale is glauconitic
Upper Cretaceous Habur ^y	Sandstone, Shale
Lower Cretaceous Aptian Habur ^{a,b,c,d,f,m,q,v,5,11,12} /Abur ^s /Hapur ^w	Arenaceous limestone and calcareous, coquinooidal limestone, shale
Aptian – Coniacian Habur ^o	
Neocomian Pariwar ^{a,b,c,d,e,f,g,o,p,q,u,v,w,x,y,z,1,2,3,7,8,11,12,13}	Sandstone and shale alternation with plant fossils, fossilised tree trunk, clean coarse sandstone, argillaceous sandstone, dominantly clean sandstone medium to fine compact with interbeds of shale, occasionally lignite present
Valanginian – Barremian Parihar ^s	Grit, gritty sandstone, quartzose sandstone, unfossiliferous
Upper Jurassic Baisakhi/ Bhadasar ^{a,c,d,e,g,x,y,z,1,2,3,7}	Sandstone and Shale, Clay, alternate layer of fissile, pyritic, micaceous shale and medium to fine sandstone, alternations of fine dirty white, feebly calcareous sandstone and grey carbonaceous shale, micaceous shale at the middle part, base is marked by brownish grey, silty glauconitic claystone
Kimmeridgian – Tithonian Baisakhi/ Bhadasar ^{8,13}	Alternations of fine dirty white to light grey, feebly calcareous and pyritic sandstone and dark carbonaceous shale, base is marked by brownish grey glauconitic shale.
Tithonian/ Portlandian Bhadasar ^{b,f,m,o,p,q,v,w,11,12} ,Bedesir ^{u,x,y} Mokal ^{a,b,p} Kolar Dunger ^{a,b,j,p,9}	Coarse to fine-grained sandstone, marine in the lower part grading into nonmarine sequence at the top, sandstone above and shales below, nodules bearing trace fossils, argillaceous sandstone, shale. Sandstone and limestone.alternation of ferruginous gritty sandstone and cemented sandstone beds with intercalations of calcareous clay.
Kimmeridgian	Marine shale and sandstone alternations, intercalated fine grained argillaceous sandstone and grey shales, hard argillaceous sandstone, grey to black shale, gypseous clay streaks, sandy siltstones, hard quartzose, silty glauconitic clay.
Baisakhi ^{b,i,m,o,p,q,u,v,11,12} Rupsi ^{b,p} Ludharva ^{b,p} Baisakhi ^{b,p} Bhadasar ^{k,l}	
Early Cretaceous Mokal ^{k,l}	
Tithonian Kolar Dunger ^{k,l}	
Upper Jurassic Bedesir ^s	Grit, sandstone and shale
Tithonian – Oxfordian	Grey to black shale commonly ferruginous in nature and rare remains of plants
Baisakhi ^{k,l,9} Lanela ^{a,k,l,9} Ludhawra ^{a,k,l,9}	

(continued)

Table 1. Continued.

Age/Series/Formation	Lithology/key features
Rupsi ^{a,k,l,9}	Brown hard argillaceous, sandstone and intraformational conglomerate.
Basal ^{k,l,9}	shale of grey to greenish colour which is intercalated with sandstone of light brown colour.
Kimmeridgian-Middle Oxfordian	Sandstone and gypseous shale
Baisakhi ^{j,5}	
Late Kimmeridgian	
Lanela ^j	
Middle Kimmeridgian	
Ludhawra ^j	
Early Kimmeridgian-late Oxfordian	
Rupsi ^{j,n}	
Late Oxfordian	Limestone, shales, lower part carbonaceous.
Basal ^j	
Middle Jurassic	
Bajocian – Oxfordian	
Jaisalmer ^{a,b,c,d,e,f,g,i,j,k,v,w,x,y,z,1,2,3,4,7,11,12}	Alternations of marine arenaceous limestone and calcareous sandstones, at places oolitic and bioclastic towards the bottom, dominantly buff to grey, hard and compact limestone interbedded with fine to medium grained calcareous sandstone and shale.
Late Callovian – Oxfordian	
Kuldhar ^{b,f,l,4}	Argillaceous, ferruginous silty and oolitic limestone types; oolitic shale, gypsiferous clays and sandstone. Typical Section: Kuldhar Nala section
Middle Callovian	
Badabag ^{b,l,4}	Cross-bedded calcareous sandstone, dolomitized sandy limestone, intraformational conglomerate, sandstone. Typical Section: Badabag hill scrap section
Early Callovian	
Fort ^{b,l,4}	Oolitic, coarse, sandy fossiliferous limestone, crossbedded sandy limestone. Fine to medium grained sandstone. Typical Section: Fort escarpment section
Bajocian – Bathonian	
Joyan ^{b,l,4}	Coquinoidal limestone gritty-sandstone, ferruginous sandstone. Typical Section: Jaisalmer to Thiat Road
Bajocian – Bathonian	
Hamira ^{b,l,4}	Sandy limestone, calcareous sandstone, and marl bands
Thiat ⁴	Typical Section: Thiat scrap and section near Hamira village
Jaisalmer ^{a,b,c,d,e,f,g,j}	Mainly shale and limestone with colites
Kuldhar ^{b,f,i}	Mainly limestone
Jaisalmer ^f	
Jaisalmer ^{a,b,c,d,e,f,g,i,j,k,l,n,9,10}	
Middle Oxfordian-Early Oxfordian	
Jajiya ^{a,j,k,l,n,6,9,10,14}	Oolitic, bioturbated and cross-bedded limestones with hardgrounds and sandstone, alternating limestone and shelly limestone, golden oolite, and marly limestone. Yellow oolitic bioturbated and cross-bedded limestone and sandstone
Callovian	
Kuldhar ^{a,j,k,l,n,6,9,10,14}	Oolitic limestone, fossiliferous, oolitic silty marls, shell beds, shales and limestones, Yellow limestone, greenish shale, and golden oolite, fossiliferous oolitic silty marl, shell beds, shales
Late Bathonian	Siltstones, sandstones, well cemented shelly and sandy limestones with hardgrounds and intraformational conglomerate. Yellow and buff limestone, shelly limestone, yellow sandstone, greenish shale and conglomerate, marl mudstone
Badabag ^{a,j,k,l,n,6,9,10,14}	
Middle Bathonian-Early Bathonian	Poorly to moderately cemented sandstones, fossiliferous bioturbated to cross-bedded limestones, Buff, yellow to greenish yellow limestone, and soft, light coloured sandstone
Fort ^{a,j,k,l,n,6,9,10,14}	
Bajocian	

(continued)

Table 1. Continued.

Age/Series/Formation	Lithology/key features
Joyan ^{a,j,k,l,n,6,9,10,14}	Cross-bedded limestones with erosional surfaces and reworked large coral heads, bioturbated limestones and fine-grained sandstones. Shelly limestone, marl, shale and sandstone
Hamira ^{j,k,l,n,6,9, 10,14} Oxfordian – Callovian	Cross-bedded calcareous sandstones. Yellow arenaceous limestone, shale and marl
Jaisalmer ^{m,o,p,q,s,u,8,13} Kuldhar ^{p,8} Badabag ^{p,8} Fort ^{p,8}	Alternations of marine arenaceous limestone and calcareous sandstone with a top fossiliferous oolite bed, shell limestone, dominantly buff to grey tight limestone, thin intercalations of shale are common
Joyan ^{p,8} Hamira ⁸ Lower Jurassic	Mainly dirty white calcareous sandstone and intercalated shale with occasional bands of limestone.
Lias – Bajocian Lathi ^{a,b,c,d,e,f,g,j,k,l,m,n,s,v,w,x,y,z, 1, 2, 3,7,9,11,12,14}	Sandstone, shale, lignite, Plant fossils, Terrestrial to deltaic sandstone. Calcareous sandstone variegated calcareous sandy silt stone, conglomerate with fossil tree trunks in fossil tree trunks in coarse sandstone, micaceous claystone, sandstones are medium to coarse, dirty white to grey calcareous towards top, thin intercalations of ferruginous claystone and micaceous carbonaceous shale.
Thaiyat ^{a,b,j,k,l,n,9,14} Oдания ^{a,b,j,k,l,n,4,9,14} Lias – Bathonian Lathi ^{o,p,8,13}	Siltstones and fine-grained sandstones Cross-bedded, poorly sorted sandstones with pebbles
Thaiyat ^p Lias Lathi ^q Permo Triassic Bhuana ^{a,g,7,8,11,12,13}	Mainly sandstone medium to fine, grey to dirty white at places calcareous , thin intercalations of chocolate brown claystone and grey shales, lignite streaks Sandstone with plant fossil.
Triassic Sumarwali ^{e,f,w,3}	Sandstone red, brown and pink, claystone and shale, sandstones coarse to medium with intercalations of ferruginous claystone and shale.
Permian Karampur ^{e,w,3}	Sandstone and clay stone
Permo-Carboniferous Badhaura Formation ⁵	Shale and sandstone
Proterozoic – Lower Cambrian Cambrian Birmania ^{a,e,v,3,11,12,13}	Carbonate, dolomitic limestone, shale and sandstone
Neoproterozoic Tonian/Cryogenian Randha ^{a,e,v,3,11,12} Basement ^{e,v,7,11,12,13}	Calcareous quartzite, sandstone and shale Malani igneous suite/metamorphic basement, Phyllite, Schist, Granite

References:

- aZadan and Arbab (2015),
bRai and Garg (2007),
cAhmad and Aquil (2000),
dVerma et al. (2012),
ePandey et al. (2019c),
fKrishna Brahman (1993),
gSingh et al. (2006),
iMahender and Banerji (1990),

jSaha et al. (2021),
 kAlberti et al. (2017),
 lSharma and Pandey (2016),
 mMude et al. (2012),
 nPandey et al. (2012),
 oTorsvik et al. (2005),
 pSudan et al. (2000),
 qDas Gupta (1975),
 rKalia and Kintso (2006),
 sAlam (1993),
 tBhandari (2008),
 uSigal et al. (1971),
 vPatra and Singh (2015),
 wAwasthi (2002),
 xMitra et al. (1993). ^y Sinha et al. (1993),
 zLal (1994),
 1Chidambaram (1991),
 2Upadhyay (1991),
 3Singh (2000),
 4Ahmad et al. (2013),
 5Bafna and Dhaka (1999),
 6Kachhara and Jodhawat (1999),⁷ Srivastava and Pandey (1996),⁸ N.P. Singh (1996),
 9Ahmad et al. (2022),
 10Kaur et al. (2020).
 11Asher et al. (2021)
 12Zutsi and Panwer (1997)
 13Bhadu and Mondal (2018)
 14Kalita (2015)

Phanerozoic geologic evolution of the basin initiated when the Indian plate separated from Gondwana (Torsvik et al. 2005) during Jurassic and Cretaceous. The NE-SW and NW-SE fracture systems reframed the Jaisalmer basin whereby the oldest rocks crop out as the Habur Formation (Pandey et al. 2019c). The major evolution of the Jaisalmer basin initiated in Mesozoic after a hiatus and commenced as the fluvio-deltaic deposition of the Lathi Formation (Srivastava 1966). The Jaisalmer basin lies uncomfortably over the Proterozoic basement. The Malani igneous suits and the Precambrian metamorphic rock constitute the basement of the Jaisalmer Basin (Table 1). The basin consists of alternating sequences of clastics and carbonates. Table 1 compiles the stratigraphy of the Jaisalmer basin. Well-exposed Mesozoic rocks are mapped as six formations (Lathi to Habur Formation; Zadan and Arbab 2015). As per Awasthi (2002), sedimentation in the Jaisalmer basin started during Permian with shallow marine deposition of the Karampur Formation.

Ramgarh fault, Ghotaru fault, Kanoi fault and Fatehgarh fault are the major faults of the study area. The first three of them have overall NW trend whereas Fatehgarh fault trends NE-SW. Between the Ramgarh and the Kanoi Faults, Manhera Fault and Manhera Tibba structure exist along with the Kharatar structure (Alam 1993; Ahmad and Aquil 2000; Roy and Jakar 2002; Ahmad et al. 2013; Singh 2007; Figure 1A).

Several closure or flexural structures occur in the study area (Figure 1A; Das Gupta 1975), which are the major hydrocarbon producing structures formed due to strike-slip tectonics (Mitra et al. 1993; Pandey et al. 2019b).

3. Methods

3.1. Meso-scale study

The tectonic processes are reflected by stream networking systems and manifest as morphotectonic characters of the watersheds. Weights have been assigned to basic relief,

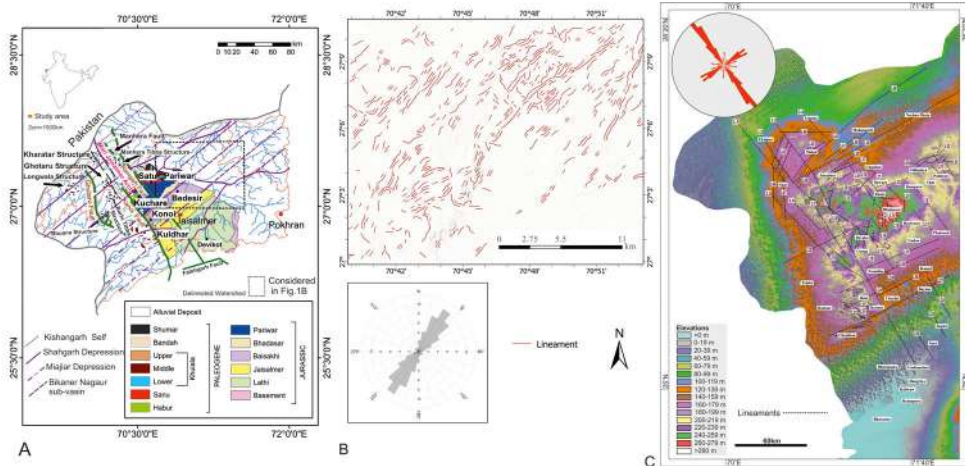


Figure 1. A. Geologic formations with major fault lines and structures of Jaisalmer basin (Pandey and Chowdhury 2010). Watersheds have been delineated in this basin. B. Analysis and superposition of lineaments extracted from multi-look C-band SAR data with bi-directional rose diagram representing the lineaments. C. Fifty-three lineaments have been identified from DEM in the Jaisalmer-Barmer area. Most of them strike NW-SE (inset rose diagram).

drainage and morphometric techniques that characterize channel and watershed-scale geometries. These indicators cumulatively constrain the tectonic activity of the watersheds of the basin. Exercise of integrated morphometric techniques and geometric data analysis are computed using the Digital Elevation Model (DEM) of the Bhuvan Cartosat 1 (30 m resolution), 2015.

The stream network system extracted from the DEM. This is based on flow path, the direction at each point on the topographic surface tracing towards the downhill water flowing path, and the crossing contours. Considering (i) streamline tracing and (ii) flow direction based on steepest descent, the slope directions from each pixel to its eight-neighbour pixels have been framed. Streamlines were generated and extracted using the D8 Python algorithm adopting the required threshold value. Discrete flow angles and single flow direction are applied to delineate the watershed boundaries.

The extracted drainage lines are in the Google Earth Pro in Arc 10.3 platform. We incorporate relief characteristics, and drainage and morphometric parameters for each watershed. The considered indicators for index of relative active tectonics (IAT) are verified by applying the Analytic Hierarchic Process (AHP) analysis in calculating weight.

AHP has been used to calculate the weight for each of the parameters used to identify the tectonic effects over the rivers. AHP is a multi-criteria decision-making method introduced by Satty (1980). First, pair-wise comparison matrix was prepared as per the Satty Scale (Table 2).

Consistency Index (CI) is calculated (Liu et al. 2017):

$$CI = \frac{\gamma_{Max} - n}{n - 1} \tag{1}$$

$$CR = CI - RI \tag{2}$$

Here CI: consistency index; consistency ratio CR; RI: random consistency index; γ_{Max} : computed average value of weight; n: number of parameters. There is a randomly generated comparison matrix (Satty scale 1980, Liu et al. 2017). CR has been computed to check the consistency of the judgement matrix. As per the Satty scale, for $CR \leq 0.10$, the matrix can be marked with satisfactory consistency.

Table 2. Applied linear & spatial scale methods to analyze tectonic signatures.

Sl. No.	Indices	Relief characterizes	Reference
1.	Elevation map	Extracted from DEM in Arc GIS10.3	NA
2.	Slope Map	Extracted from DEM in Arc GIS10.3	NA
3.	Aspect Map	Extracted from DEM in Arc GIS10.3	NA
Sl. No.	Indices	Drainage analysis	Reference
1.	Drainage Density	$D_d = L_u/A$ (Extracted from DEM in Arc GIS10.3.) L_u – Total stream length, A-Total area	Horton (1945)
2.	Stream Order	Hierarchic order.	Strahler (1952); Rai et al. (2017)
3.	Drainage Pattern	Extracted from Drainage map	Morisawa (1985)
Sl. No.	Indices	Morphometric parameters	Reference
1.	Normalize long profile	The linear function $y = ax + b$ The logarithmic function $y = a \ln x + b$ Where, y is the elevation (H/H ₀ ; H = elevation of each point, H ₀ = elevation of the source), x is the length of the river (L/L ₀ ; L = distance of the point from the source, L ₀ = total length of the stream), a and b are the coefficients derived independently from each profile. The R2 value determines the best fit. The curve with Highest R2 value is the best-fit curve. (Extracted from SRTM 30 m DEM and formulated using Arc GIS 10.4 and TNT mips 2014 platform)	e.g. Paul and Biswas(2019); Kale et. al. (2014); Lee and Tsai (2010)
2.	Concavity Index(Θ)	$C_{eh} = \frac{1}{S_2 - S_1} \Delta E$ Where, S ₁ is the channel slope prior to disturbance, S ₂ is the channel slope after disturbance (e.g. due to a change in incision rate E) and ΔE is the difference between the incision rate before and after disturbance.	e.g. Whipple et al. (2007); Wobus et al. (2006)
3.	Stream Gradient Index (SL)	$SL = \frac{f}{\ln D_2 - \ln D_1}$ Where, f = fall in elevation (e ₂ -e ₁) ln = Natural logarithm of the cumulative distance *Higher SL value indicated tectonic control over stream.	Hack (1957)
4.	Hypsometric Integral (HI)	$HI = \frac{(H_{mean} - H_{min})}{(H_{max} - H_{min})}$ Where, H mean = Mean elevation of the basin, Hmin = Minimum elevation of the basin, Hmax = Maximum elevation of the basin. HI value ≤ 0.30 states tectonically stable basin and ≥ 0.30 indicated tectonically unstable basin.	Strahler (1952); Schumm (1956); Andreani et al. (2014)
5.	Transverse topographic symmetry factor (T)	$T = \frac{D_d}{D_a}$ Da = distance between the midline of the drainage basin and the active meander belt midline and Dd = distance between the midline and the basin divide. If the river flows through the midway of the basin, the resulting (T) would be '0' indicates symmetric basin. If the value is > 0, the river basin is asymmetric.	Cox (1994); Sajadian et al. (2015); Takieh et al.(2015)
6.	Sinuosity Index (SI)	$SI = \frac{\text{Channel Length}}{\text{Valley Length}}$ Straight channel values <1.05 Straight to Sinuous values between	Biswas and Dhara (2019); Miall (1977); Brice

(continued)

Table 2. Continued.

Sl. No.	Indices	Relief characterizes	Reference
		>1.05 - <1.50 Meandering channel indicates >1.50	(1964); Schumm and Khan (1972);
7.	Basin shape Index (B_s)	$B_s = \frac{B_l}{B_w}$ Where, B_l = Length of the basin and B_w = Width of the basin measured at its widest part. Greater the B_s value, more tectonically active basin representing its elongated shape. Lower the B_s value, the basin is tectonically less active representing the circulatory shape.	Bull and McFadden (1977); Ramírez-Herrera (1998)
8.a	Basin Perimeter,	Computed by Arc GIS software 10.3.1 using SRTM data 30 m.	NA
8.b	Basin Area,		
8.c	Basin Length.		
9.	Elongation Ratio (Re)	$Re = 2 / L_b * (A / \pi) 0.5$ Where, L_b = Length of the river basin A = Area of the river basin <ul style="list-style-type: none"> • Circular (0.9–0.10), oval (0.8–0.9), less elongated (0.7–0.8), elongated (0.5–0.7), and more elongated (< 0.5). • 0.9–1.0Circular 	Schumm (1956) Pareta and Pareta (2011); Rai et al. (2017)
10.	Tilt Angle	0.8–0.9Oval 0.7–0.8Less elongated <0.7Elongated $\beta = \arccos \left[\sqrt{\left\{ \left(\frac{b}{a} \right)^2 \sin^2 a + \cos^2 a \right\}} \right]$ Where, a = average slope, a = half of the length of the major axis, $b = b$ is the half of the length of the minor axis.	Mandal and Sarkar(2016)

IAT is a function of a number of other indices that provides reliable semi-quantitative assessments of the relative degree of tectonic activeness (e.g. Kale et al. 2014; Mahmood and Gloaguen 2012; Biswas et al. 2022; Dasgupta et al. 2022; Surabhi et al., submitted). These individual indices are Basin shape index (B_s), Transverse Topographic Symmetry Factor (T), Hypsometric Integral (HI), Elongation Ratio (Re), Circularity Ratio (Rc), Tilt angle (β) and Form Factor (Rf). These parameters have been clubbed as: class-1(High), class-2 (Moderate) and class-3 (Low) (Tables 3 and 4).

3.2. Micro-scale study

Appendix presents the data sources and the software used in this work. We calculated the following parameters for fluvio-morphometric studies.

Drainage Basin Asymmetry (AF) (Hare and Gardner 1985):

$$AF = (Ar/At) \times 100 \tag{3}$$

Here Ar : basin area on the right, and At : total basin area.

Table 3. Calculated values of different Basin scale parameters of 4 considered watersheds with their classification.

Parameters	Circularity Ratio (Rc)	Form Factor (Rf)	Elongation Ratio (Re)	Hypsometric Basin shape		Transverse Topographic	
				Integral (HI)	Index (Bs)	Tilt Angle (β)	Symmetry Factor(T)
Watersheds							
Watershed 1	0.18	0.44	0.75	0.39	1.88	2.398	0.21
Watershed 2	0.14	0.55	0.83	0.37	1.27	1.994	0.15
Watershed 3	0.11	0.31	0.62	0.28	2.19	2.548	0.57
Watershed 4	0.16	0.2	0.51	0.46	3.72	2.748	0.68
	Classification						
Class 1	0.10–0.12	0.20–0.32	0.51–0.61	0.41–0.46	3.09–3.99	2.16–2.91	0.62–0.87
Class 2	0.13–0.15	0.33–0.45	0.62–0.72	0.35–0.40	2.18–3.08	2.30–2.60	0.36–0.61
Class 3	0.16–0.18	0.45–0.58	0.73–0.83	0.28–0.34	1.27–2.17	1.99–2.29	0.10–0.35

Table 4. Ranking of calculated values for the assessment of IAT and classification of tectonic activeness amongst the watersheds.

Watersheds	Circularity Ratio(Rc)	Form Factor(Rf)	Elongation Ratio(Re)	Hypsometric Basin shape		Transverse Topographic		IAT
				Integral (HI)	Index (Bs)	Tilt Angle(β)	Symmetry Factor(T)	
Watershed 1	3	2	3	2	3	2	3	2.571429
Watershed 2	2	3	3	2	3	3	3	2.714286
Watershed 3	1	1	2	3	2	2	2	1.857143
Watershed 4	3	1	1	1	1	1	1	1.285714
Classes	Value range		Tectonic activeness					
Class 1	1.25–1.75	High						
Class2	1.76–2.26	Moderate						
Class3	2.27–2.77	Low						

Valley floor width to height ratio (V_f) (Anand and Pradhan 2019):

$$V_f = \frac{2V_{fw}}{[(E_{ld} - E_{rd}) + (E_{rd} - E_{sc})]} \tag{4}$$

Here V_f : width of the valley floor, E_{ld} and E_{rd} : elevations of the divide on the left and right side of the valley, respectively. E_{sc} : average elevation of the valley.

Hypsometric Curve Analyses (Strahler 1952; Hamdouni et al. 2008; Smith et al. 2009; Anand and Pradhan 2019) were performed using percentage method with two ratios: (h/H) and (a/A). Here a : area within a given contour, A : total area, h : elevation of that contour from the lowest point in the basin, and H : relief of the basin.

The geomorphic cycle of the basin is presented in terms of young, mature and old stage of the basin development. These three stages can be linked with tectonics. Strahler (1952) initiated such studies, which has been furthered by several workers (e.g. Hamdouni et al. 2008; Smith et al. 2009; Anand and Pradhan 2019).

Regression analyses of the Stream Longitudinal Profiles utilized the following formulae:

$$\text{LinearRegression : } y = mx + b \tag{5}$$

$$\text{ExponentialRegression : } y = ae^{bx} \tag{6}$$

Micro-scale study was performed at three spots to decipher the morphologic expressions for lineaments and faults. With details of tectonic map, three spot studies have incorporated with their elevation profiles for all these spots. Data have been extracted from Google Earth pro images and processed in Surfer 15 (ver. 2017) and Arc GIS 10.4 platform (2016).

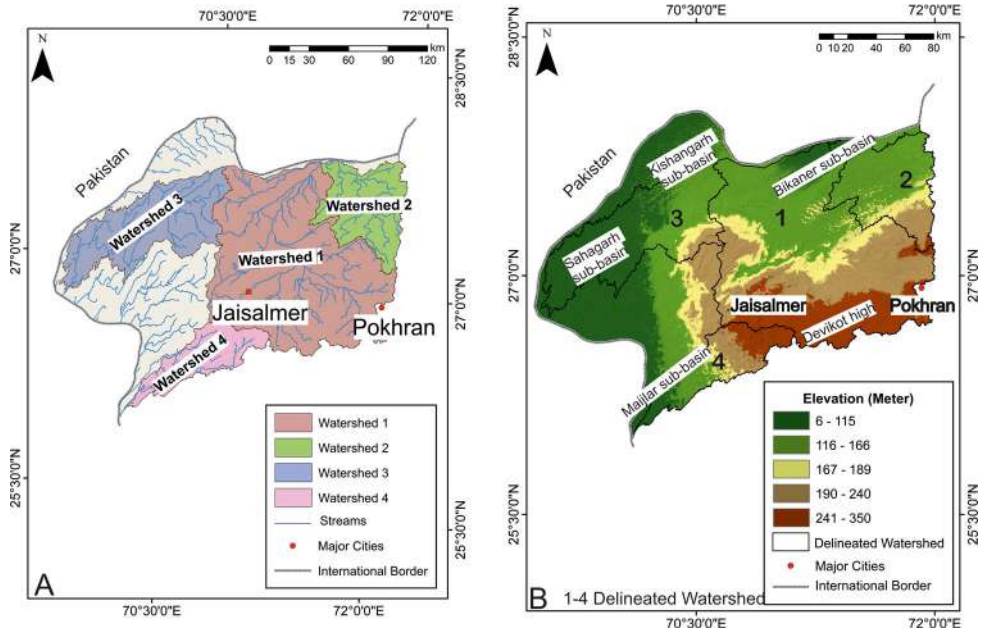


Figure 2. A. Cartosat 1 DEM based four delineated watersheds of the Jaisalmer basin. B. Elevation map of the area where south-eastern part is mostly elevated, belongs to the Devikot high and south-western arc-shaped region is less elevated, filled up by alluvium deposits.

It is a geomorphological work but morphological photos, and/or structures are not added from field. Due to the COVID situation, we were unable to do field work. The work is based on Remote sensing and morphotectonic quantification.

4. Results

4.1. DEM analysis (meso-scale study)

DEM reveals mainly NE-SW, ENE-WSW/E-W and NNW-SSE trending lineaments (Figure 1B). Fifty-three lineaments of the Jaisalmer basin (and its adjacent Barmer basin) were extracted from the remote sensing data (Figure 1C). NW-SE trend is revealed in the rose diagram (inset in Figure 1C).

Four drainage watersheds (Figure 2A) were defined to establish the role of basement tectonics with reactivation of the sub-surface structure (Pati et al. 2006) that control the topographic slope variation. Few drainage lines were not possible to take under any watershed, but they characterize the active tectonics, and are located near the Manhera fault at NW and SW parts of the basin (Figure 1A). However, in Figure 2B the elevation map presents the regional topographic variation from the Devikot high in the east to the Kishangarh sub-basin in NW and Shahgarh Sub-basin in SW.

Characterization of spatial slope segments and their directions represent the aerial surface topology that induced the flow paths of channels. The aspect slope map denotes the direction of slope with elevated flat and plain surfaces, and therefore is comparable with slope map in degree (Repository Figure S1A,B). Slope map ranging from 1.34° to 40.83° covers mostly the watersheds 1, 3 and 4. It has the capability to apparently reflect (sub-surface) structures, faults and lineaments, which in turn control the topography. Watershed 3 and parts of 1 and 4 have higher slope ($> 9^{\circ}$). The remainders are of lower

magnitude within 1.5° . The accumulation of huge parabolic and parallel dunes in NW and SW parts of the basin impose gentle slope.

The displacements of the Kanoi and Ramgarh faults create steep sides with a higher slope of the watersheds. The elevated part is named as the Devikot high. Here basins/watersheds/channels are related to rivers. In this article, we denote river watersheds as watersheds or basins. The Jaisalmer basin has been designated as a tectonic basin. This article makes primarily a geomorphologic analysis of the Jaisalmer basin and do not directly comment about hydrocarbon exploration issues.

Stream order is a measure of the position of a stream in its hierarchy position of the tributaries (e.g. Prakash et al. 2017). The stream classification is based on the master stream with several tributaries defining stream-order and drainage coverage area (e.g. Strahler 1957; Prakash et al. 2017). Watersheds 1 and 3 consist of fourth-order streams, and 2 and 4 are under the third-order category. As per Horton's law, the number of streams decreases with geomorphic progression with increase in the stream-order (Figure 3A; Prakash et al. 2017).

Analysis of drainage pattern can constrain orientation of structures viz., faults, shear zones, lineaments and folds (Ansa and Mangold 2006). Large extents of interleaved dendritic drainage patterns develop in fractured, equally resistant (Flugel et al. 2015) and homogeneous lithologies with (sub)horizontal strata (Prakash et al. 2017). In watersheds 1, 2 and partly in 4, dendritic pattern is well developed over the Devikot high. A rectangular pattern indicates regular right-angled joint/fault sets in the rock. In the middle part of watershed 3, rectangular drainage pattern is identified where the NW-trending Ghotaru fault passes and is distinctly separated by the Kharatar structure from the upper course of the basin.

The upper course of the watershed-3 is highly controlled by faults and lineaments viz., Manhera fault, Manhera Tibba structure, NW-SE parallel Ramgarh and Kanoi faults and the Mari Jaisalmer Arch in between. The complex structural pattern has controlled the drainage into a trellis pattern. Here the main streams are more wide-spaced possibly defining 'fault trellis pattern' (e.g. Drummond and Erkeling 2014). In the southeastern part of Jaisalmer town, complex barbed pattern has developed in watershed 1 where streams join in a hook-like junction indicating stream piracy. Here the SW-NE extended Kanoi fault and the Barhi Tibba structure exist as the water divide for the NE-SW flowing channels. The barbed pattern has developed typically in the Jurassic Baisakhi and the Jaisalmer Formation (Figure 3B).

Figure 4A presents the drainage densities of the basin area considering each watershed separately. All the watersheds drainage density values increase up to 0.46, and are inversely related to elevation. Minimum drainage density values occur near the water-divide and are followed by higher value towards downstream where several tributaries join at a different angle and direction as per the slope. The terrain at higher elevation in the eastern part of the basin consists of low drainage density values, which covers the area of the water divides from where two sets of drainage system originated with opposite flow directions as watersheds 1 and 4. A minimum drainage density value of 0.07 comes out where the Mari-Jaisalmer arch is elevated and E-W elongated between the Rangarh fault and the Kanoi fault. This arch behaves as a water divide from where the drainage lines spread out.

The morphometric indices provide a noticeable difference in values for the considered four watersheds of the study area. The accuracy level in selecting the parameters for IAT is verified with the application of AHP where individual indicators have given individual weight with rank 1 to be tectonically active. Thus $CI = 0.099304$ and $CR = 0.088133$,

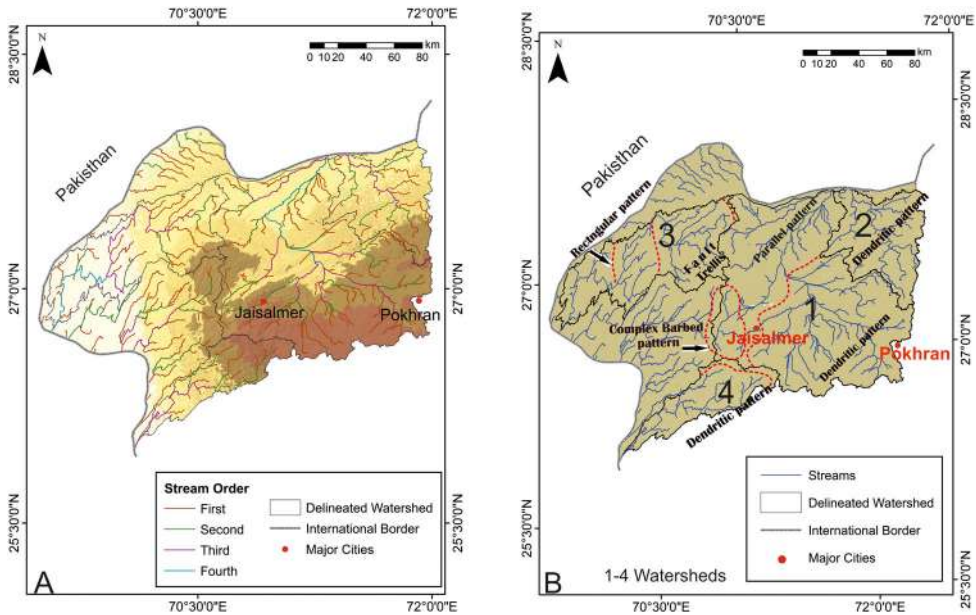


Figure 3. A. Stream order map of the study area where the watershed 3 and 1 are the fourth-order stream, and watersheds like 2 and 4 are the third-order stream. Stream-order defines the stream frequency number in different order. B. Drainage pattern map of the four watersheds where rectangular, fault trellis, complex barbed and dendritic pattern are marked in red dotted lines.

both < 1 , indicate the judgment matrix with satisfactory consistency. It is essentially applied to ensure that the given weight for the indicators is absolutely accurate for further calculations (Figure 4B,C).

The relatively young drainage basins in terms of active tectonics can be constrained in terms of the basin shape Index (B_s). A basin parallel to the topographic slope indicates that it is tectonically active. The widths of the watersheds reduce where the energy of the stream primarily evolve with vertical incision near the tectonically active areas. In contrast, rapid uplift disrupts where the valley widens by lateral erosion in the less active flat terrain common in downstream area with lower slope. The range of B_s values (3.09–3.99) is higher in watershed 4 where the Kanoi fault exists as the evidence of active tectonics, which decreases in watershed-3 (2.18–3.08), and in watersheds 1 and 2 (1.27–2.17). The northwestern part of watershed 1 and the entire watershed 2 has less elongated geometries.

Elongation ratio (Re) is the ratio of the diameter of a circle of the same area of the watershed to the maximum length of the basin/watershed. Values close to 1 distinctly signify the regions characterized by very low relief, gentle slope and less undulation as watersheds 1 and 2 (0.73–0.83). Values towards '0' indicate a more elongated watershed located on a steeper slope in the area. The specific detection of slope with ground is slant in watershed 3. Re for watershed 3 ranges 0.62–0.72, and in watershed 4 it is 0.51–0.61. As uplift stopped, watersheds became circular in tectonically-controlled areas (Singh et al. 2015). $Re < 0.7$ indicates the watershed to be tectonically active. $Re > 0.7$ connotes a stable watershed.

The hypsometric integral (HI) represents the elevation distribution of the watershed/landscape. It is comparable with the stream length gradient index where rock strength matters. Stream length (SL) index defines gradient within a short stretch. Where the slope

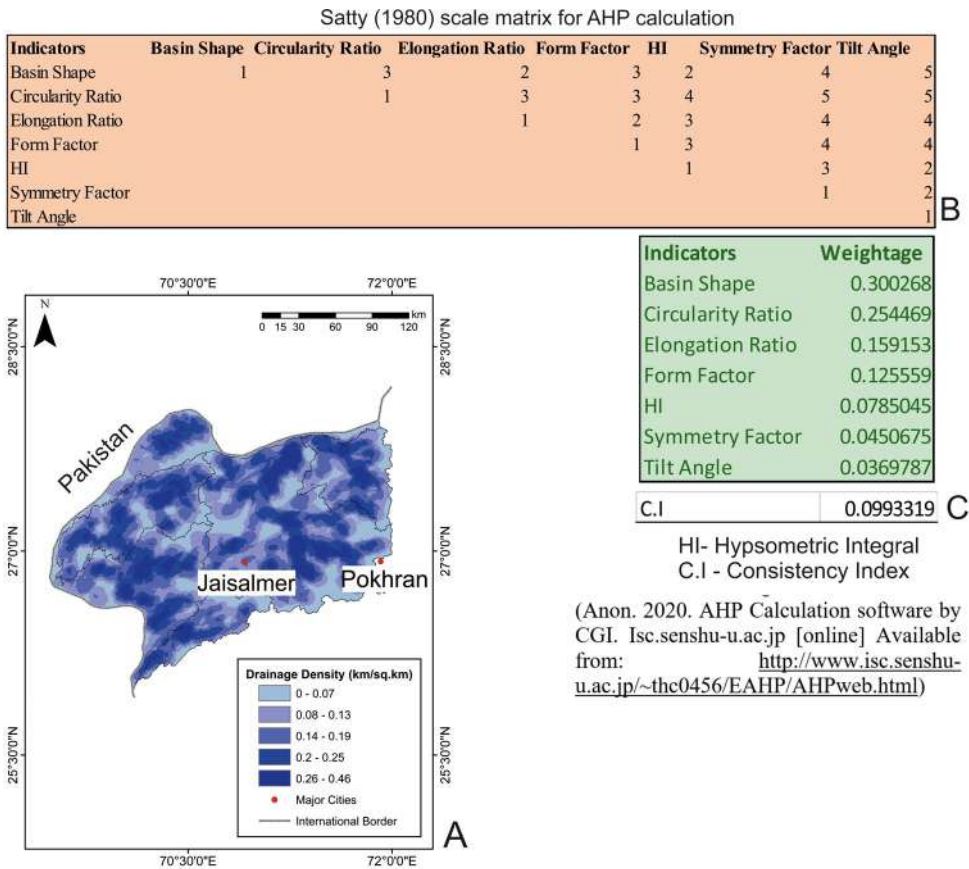


Figure 4. A. Drainage density map of the watersheds ranging between 0.07 and 0.46 km/km⁻². B, C. Matrix calculation of the considered parameters for AHP calculation and computed weight of each indicator with result of the Consistency Index used to calculate IAT.

is steep and gradient become gentle, SL values become low (Moussi et al. 2018). Higher the range of HI as in watershed 4 (0.41–0.46), lesser is the erosion in the upland. This could indicate a younger landscape (e.g. Mahmood and Gloaguen 2012; Czerniawska and Chlachula 2018). A highest range of HI (0.41–0.46) in watershed 4 denotes the effect of recent incision over the geomorphic surface. The upper part of the catchment is made up of Joyan Member, Fort Member and Badabag Member belonging to the Jaisalmer Formation and is affected by Kanoi fault (Zadan and Arbab 2015). The Hi values are categorized as class-1 (0.41–0.46), class-2 (0.35–0.40) and class-3 (0.28–0.34). Watershed 4 is less eroded (under class-1) and exists in an active young stage.

The parameter Circularity Ratio (Re) displays the degree of circular shape of the watershed and indicates the uniform infiltration/seepage in long time with respect to slope. In the study area, sand covers watershed 3. This watershed gives a low range of Re (0.10–0.12) indicating a uniform infiltration, which is followed by watersheds 2, 1 and 3. Generally, topography having low circularity ratio generates dendritic drainage pattern such as watershed 2 (Repository Figure S2D), but due to the presence of Ghotaru fault and the Longewala structure, rectangular drainage pattern has also formed locally (Figure 1A).

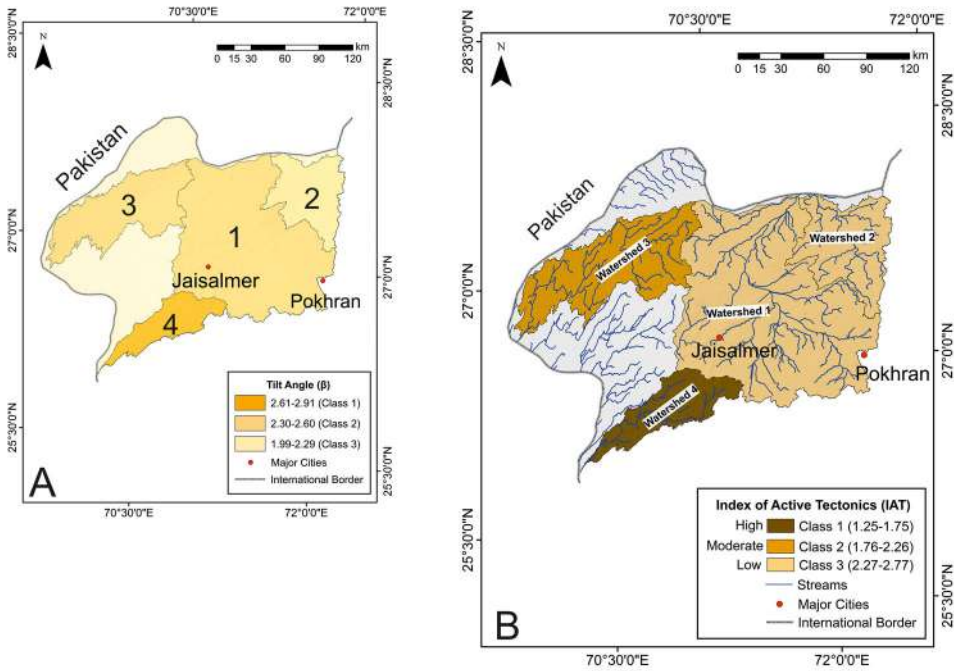


Figure 5. A. Spatial distribution of tilt angle values ranging from 1.99 to 2.91. B. Map of IAT where watershed 4 is tectonically active, followed by 3, and watersheds 1 and 2 are less active.

Form factor (R_f) defines the ratio between the river basin area to the square of the basin length, which represents the topography. Lower the R_f more elongated is the river basin with steep slope ($\sim 9.48\text{--}40.83^\circ$). R_f values in watersheds 3 and 4 under class-1 indicate steep topology related to Kanoi and Ghotaru faults. Another point, watershed 1 is moderately steep (according to the moderate class with $R_f=0.32\text{--}0.45$) where both Rangarh and Kanoi faults exist with the Mari Jaisalmer arch in between; and watershed 2 under class 3 has gentler slope (70% area under up to $\sim 2.97^\circ$).

Transverse topographic symmetry factor (T) is the ratio between the lengths of midline of the drainage basin to the midline of the active meander belt with space from the midline to the basin/watershed limit (Cox 1994). T lies between 0 to 1. $T=0$ denotes a perfectly symmetric basin, whereas values towards 1 indicate increasing asymmetry. Watershed 4 is under class-1 ($T=0.62\text{--}0.87$) and is highly asymmetric, Watershed 3 ($T=0.36\text{--}0.61$) is moderately asymmetric, and watersheds 1 and 2 ($T=0.10\text{--}0.35$) are near symmetric. Asymmetric watershed 4 is more active as it is more tilted due to tectonic control than the watersheds 3, 1 and 2 (Repository Figure S2A-F)

The tilt angle (β) represents segments of slope with their long axes oriented parallel to the direction of tilting of the watershed. It has computed from the contours generated from the DEM of the surface. Lower β represents a gentler slope. This indicates a tectonically less active watershed. A high value of β represents structure-controlled higher tectonic activity. Watershed 4 has a higher range of β (2.61–2.91). Watersheds 1 and 3 are moderately active and under class 2 with $\beta=2.30\text{--}2.60$. Watershed 2 is mature and stable with $\beta=1.99$. It comes under class 3. Considering the aspect map and slope map, 60% area of this watershed is flat with a slope $\leq 2.97^\circ$ (Figure 5A).

Calculation of the index of active tectonics (IAT) utilizes the seven geomorphic indices (B_s , T , H_i , R_e , R_c , β and R_f) for all the watersheds delineated from the Jaisalmer basin.

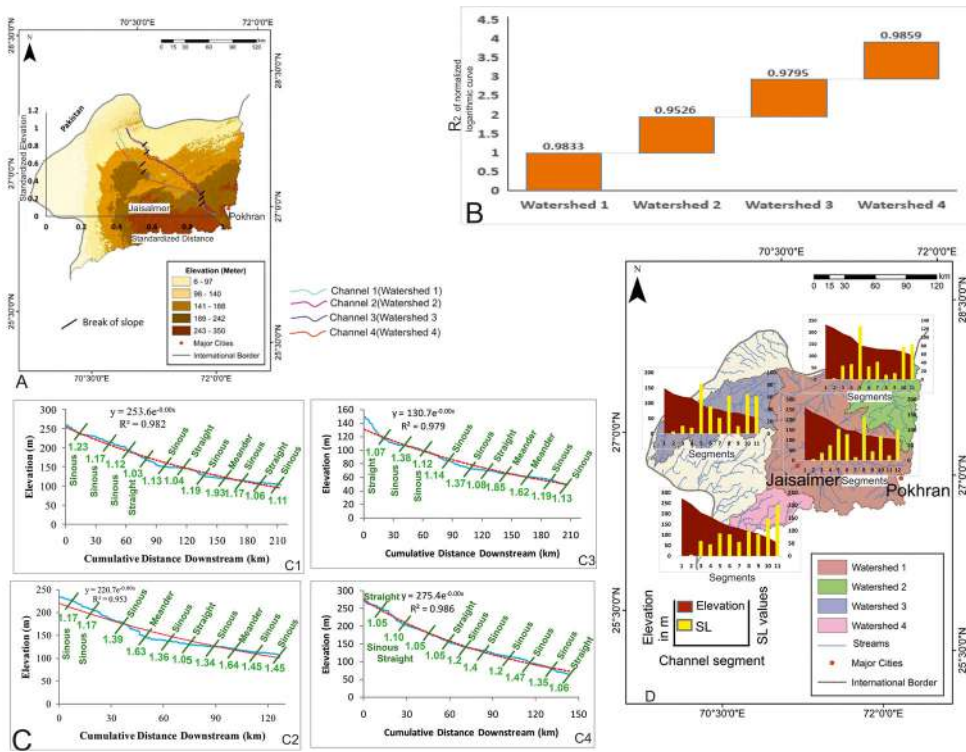


Figure 6. A. Normalized long profiles for four watersheds. Break of slope marked along the profiles indicate formation of knick points. B. Graphical representation of R^2 values indicates that these watersheds are tectonically active. However, comparing others, watershed 4 is most active, followed by watersheds 3 and 2. C. Source to mouth long profile with the displayed sinuous values along the profile address channel pattern including the probable vertical incision where the channel is straight. Alternating straight and sinuous pattern define tectonic anomalies along with the presence of lineaments and faults. D. Graphical representation of stream length gradient index (SL) with respect to elevation of watersheds 1, 2, 3 and 4, along the long profile from source to mouth.

Individual indicators address different range of clarifications that cannot provide an overall result of active tectonics. The watershed-scale parameters are arranged under three classes. Computed *IAT* results portray the active tectonics in the scale of high, moderate and low. For example, the calculated *IAT* values are grouped as class-1: 1.25–1.75 (high), class-2: 1.76–2.26 (moderate), and class-3: 2.27–2.77 (low). The spatial distribution of these values indicates that the watershed-4 comes under class-1, watershed 3 to class-2, and watersheds 1 and 2 to class-3 (Figure 5B).

This morphotectonic analysis deciphers both the linear-scale study of drainage lines and basin or watershed-scale parameters. The extracted drainage lines from the DEM represents the channel orientation, direction, alignment, angle of joining of any tributary to the master stream, and the thalweg profile of the main consequent channel. The study of profile analysis of a river system discloses the significant response to recent tectonic activities. Longitudinal profile preserves relevant information of landscape evolution with certain anomalies and abrupt changes in river gradients within the profiles. The breakoff slope along the channel indicates the tectonic anomalies revealed by rejuvenation near knick points. In the normalized steady long profiles of all the four main channels, distinct breaks in slopes have been identified that formed by localized incision. The incision is due to minor-scale local fractures along or across the channel, rock uplift and shear stress

Table 5. Results of Basin Asymmetry (AF) analyses for basins 4 to 16 of the Jaisalmer area.

Basins	A_r (km ²)	A_t (km ²)	Drainage Basin asymmetry (AF) $AF = 100 \times \left(\frac{A_r}{A_t}\right)$
4	21	39.56	53.08
5	54	77	70.13
6	38	60	63.33
7	32	61	52.46
8	145	173	83.82
9	692	1606	43.09
10	433	672	64.43
11	19	43	44.19
12	57	92	61.96
13	65	76	85.53
14	33	50	66.00
15	124	237	52.32
16	137	328	41.77

applied to the resistant lithology. These are regionally related to the major fault lines and lineaments (Figure 6A).

In Figure 6B, the comparative bar graphs of the square of the correlation coefficients (R^2) values show that the watersheds 4 and 1 are more active than 2 and 3; but overall values point out the entire watershed area as active. Therefore, it is a gradation of tectonic activeness of the considered watersheds. The normal long profile analysis with actual distance/elevation with exponential curve fit establish watershed 4 to be active and is followed by 1, 3 and 2. The calculated *SI* index in different points of the long profile represents the landscape transience and it is characterized by the valley incision and categorization of channel as straight, sinuous and meander in alternate sequence. The striking point of watershed 4, where the channel straightens from sinuous near confluence, indicates a sudden change in gradient that promoted vertical incision following the weak zone. The tectonic map of the area shows the presence of Kanoi fault (NNW-SSE), Ramgarh fault (NNW-SSE) and Fatehgarh fault (SSW-NNE). These faults occur in the upper part of the watershed 4 (Das Gupta 1975). The source area of the other channels west of watersheds 1 and 4 is straight and alters to sinuous towards downstream. Meandering occurs in the downstream section in watersheds 2 and 3. However, due to regional inversion of relief (Kar 2011), steep gradient sinuous channels developed. Therefore, the irregular vertical valley incision and lateral cutting along the channel is associated with the change in landscape adjustment with tectonic evolution (Figure 6C). These changes are analyzed according to the elevation of the channel bed from source to mouth using the *SL* index. Lower *SL* values indicate that the channel is crossing the faults (Dehbozorgi et al. 2010) and is younger than the faults. It works on river channel morphology along with tectonically derived features. Higher values of *SL* indicate the major fault lines whereas low magnitudes indicate the lineaments, fractures and minor scale faults (Figure 6D).

4.2. Micro-scale study

Based on drainage networks of the ephemeral streams, 13 micro-scale watersheds are delineated. Micro level study discloses that all the watersheds are composed of a number of sub-basins/sub-watersheds, which execute same results in morphotectonic study. This morphotectonic analysis involves both the linear-scale study of drainage lines as well as basin or watershed-scale parameters. Total 13 watersheds/basins (4–16) have been considered and Table 5 presents the results of the basin asymmetry (AF) analyses (Hare and Gardner 1985; Keller and Pinter 2002) for watersheds 4 to 16 (Figure 7A). Study indicates

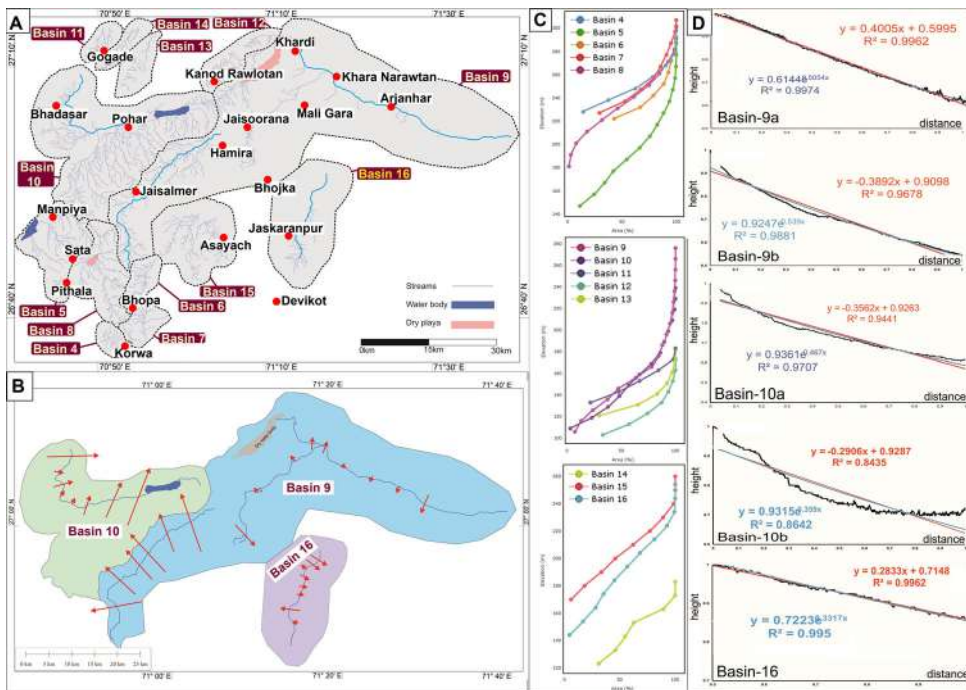


Figure 7. A. Dry gully systems identified in and around the Jaisalmer area. Drainage basins/watersheds 4 to 16 identified. Basin-9: between Jaisalmer to Jaisoorana to Arjanhar, basin-10: between Manpiya to Bhadasar to Pohar, Basin-16: near Jaskaranpur, basin-15: around Jerat. Few playas identified near Sata, Manpiya, Pohar and Deuga. B. Basin asymmetry factor (Table 5) obtained from transverse topographic symmetry analyses of basins 9, 10 and 16. C. Hypsometric curves of these basins are plotted. D. Hypsometric curves drawn for 13 basins, plotted from elevations of corresponding basins to the percentage of basin area. E. Normalised longitudinal profiles of major gullies of basins 9, 10 and 16 presented along with equations and R^2 values for linear and exponential regression analyses.

that watersheds 5, 8 and 13 are unstable with $AF > 50\%$. This may indicate presence of tectonic elements (faults or lineaments) within those watersheds (Figure 7B).

Out of the 13 watersheds, three major watersheds viz. 9, 10 and 16 are selected to calculate the valley floor to height ratio (Vf) (Kale et al. 2014) as they cover most of the drainage area of the Jaisalmer basin. As per Table 6, the main gully of watershed 10 has narrow valley in mid and upstream segments indicating rapid incision. Similarly, gully of the watershed 9 also has narrow valley upstream. Therefore, it may be inferred that upstream segments of main gullies in these two basins have narrow valley indicating presence of either resistant rock formation or lineaments.

Table 7 presents the Sinuosity Index (SI) (Brice 1964; Horacio 2014) of main gullies of the watersheds 9, 10 and 16. The data indicates presence of a meandering gully segment ($SI = 1.89$) in watershed 10, which further indicates moderate tectonic control over the morphology.

Hypsometric Curve Analyses (Strahler 1952; Zăvoianu 1985) of basins 4 to 7 are listed in Table 8, watersheds 8 to 11 in Table 9, and watersheds 12 to 16 in Table 10. The results are plotted in Figure 7C, which shows that the watershed 8 is below 300 m elevation, out of which $< 3\%$ of the total area is below 200 m, total area of watershed 9 is below 276 m, total area of watershed 10 is below 234 m elevation out of which $\sim 94\%$ area is below 200 m. Total areas of watersheds 11, 12, 13 and 14 are below 183 m elevation. Total area of watershed 15 is under 260 m elevation out which 47% area is below

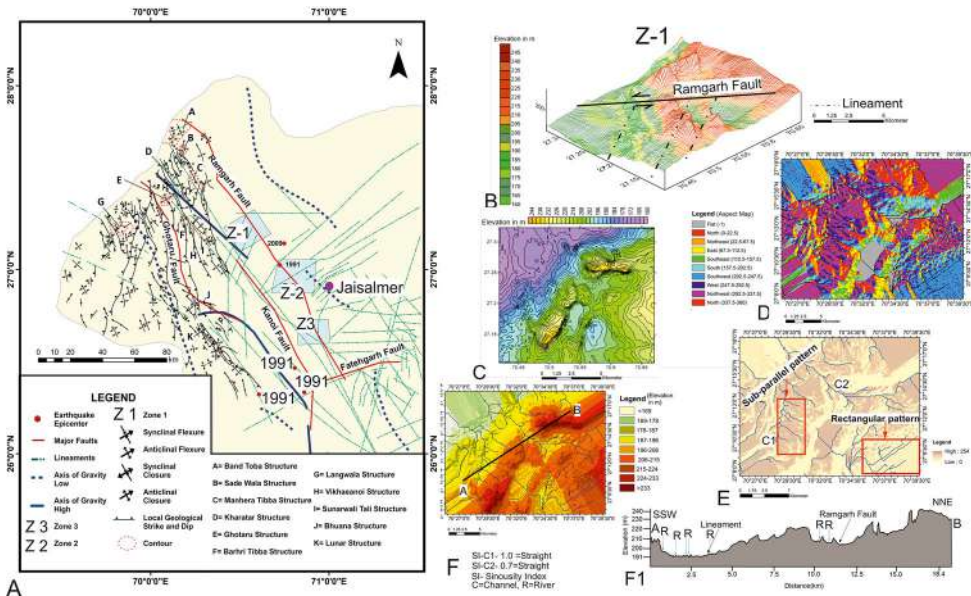


Figure 8. A.Tectonic map of the Jaisalmer and the adjacent areas. Three zones for spot study have shown.Sub-figures B-F display the details of Zone 1. B. 3D representation of zone 1 along with Rangarh fault and lineaments.C. Spatial distribution of contour pattern with elevation differentiation. D. Slope aspect map showing the slope direction of the area. E. Hill shade map of the area with detail drainage lines and identified drainage patterns. F. Absolute relief map with intersecting drainage lines and demarcation of AB line for elevation profile. F1 represents the AB section with fault/lineament and intersecting channels.

Table 6. Results for vfw for main gullies from basins/watersheds 9, 10 and 16.

Basin	Locations (Lat/Lon)	Variables	Results (Vfwh) $2V_{fw} / [(E_{ld} - E_{rd}) + (E_{rd} - E_{sc})]$
Basin 9	27° 03' 43.4249" N	$V_{fw}=519m, E_{ld}=143m$	207.60
	71° 28' 11.9754" E	$E_{rd}=145m, E_{sc}=138m$	
	27° 08' 58.0199" N	$V_{fw}=869m, E_{ld}=118m$	347.60
	71° 17' 52.1659" E	$E_{rd}=115m, E_{sc}=113m$	
	27° 04' 16.7164" N	$V_{fw}=480m, E_{ld}=130m$	192.00
	71° 09' 16.6620" E	$E_{rd}=127m, E_{sc}=125m$	
Basin 10	27° 05' 17.8375" N	$V_{fw}=1061m, E_{ld}=127.5m$	223.37
	71° 11' 51.7008" E	$E_{rd}=125.6m, E_{sc}=118m$	
	27° 03' 0.8854" N	$V_{fw}=1916m, E_{ld}=121m$	348.36
	70° 54' 10.0394" E	$E_{rd}=114m, E_{sc}=110m$	
	27° 04' 54.6599" N	$V_{fw}=627m, E_{ld}=124m$	501.60
	70° 46' 56.1620" E	$E_{rd}=123.5m, E_{sc}=121.5m$	
Basin 16	26° 58' 22.0956" N	$V_{fw}=637m, E_{ld}=155m$	127.40
	70° 51' 8.9369" E	$E_{rd}=162.5m, E_{sc}=145m$	
	26° 57' 12.0426" N	$V_{fw}=349m, E_{ld}=144m$	349.00
	70° 48' 42.5089" E	$E_{rd}=145.5m, E_{sc}=142m$	
	26° 56' 4.2878" N	$V_{fw}=340m, E_{ld}=152.5m$	194.29
	71° 16' 57.3800" E	$E_{rd}=152.5m, E_{sc}=149m$	
	26° 53' 59.8426" N	$V_{fw}=395m, E_{ld}=164m$	263.33
	71° 15' 38.6885" E	$E_{rd}=167m, E_{sc}=161m$	
26° 51' 59.3459" N	$V_{fw}=478m, E_{ld}=179m$	136.57	
71° 15' 21.2440" E	$E_{rd}=183m, E_{sc}=172m$		
26° 49' 27.6613" N	$V_{fw}=575m, E_{ld}=196m$	135.29	
71° 13' 48.6998" E	$E_{rd}=192.5m, E_{sc}=187.5m$		

200 m. Total area of watershed 16 is below 254 m out of which 68% area is below 200 m elevation. Therefore, gradient in gullies of the basins at Jaisalmer area low and the watersheds exist mostly in valleys of gentle slope with small highland catchment areas.

Table 7. Results of SI of main gullies for basins/watersheds 9, 10 and 16.

Main Gully of	Variables	Sinuosity Index (<i>SI</i>) $SI = CL/VL$
Basin 9	$CL = 55.5 \text{ km}/VL = 47.5 \text{ km}$	1.17
	$CL = 47.75 \text{ km}/VL = 34.98 \text{ km}$	1.36
Basin 10	$CL = 34.16 \text{ km}/VL = 18 \text{ km}$	1.89
	$CL = 23.42 \text{ km}/VL = 19.12 \text{ km}$	1.22
Basin 16	$CL = 22.8 \text{ km}/VL = 19.3 \text{ km}$	1.18

Table 8. Results of hypsometric curve analyses for basins/watersheds 4–7.

Basin 4		Basin 5		Basin 6		Basin 7	
Area (%)	Elevation (m)	Area (%)	Elevation (m)	Area (%)	Elevation (m)	Area (%)	Elevation (m)
14.08	228	10.94	147	42.65	222	29.05	144
37.21	238	24.07	157	66.73	232	52.60	154
62.15	248	33.85	167	78.88	242	67.09	164
78.29	258	41.90	177	88.44	252	79.39	174
90.35	268	54.21	187	92.82	262	85.66	184
97.84	278	66.19	197	95.37	272	90.91	194
99.72	288	75.60	207	98.47	282	95.08	204
100	298	82.47	217	99.94	292	98.92	214
		88.24	227	100	302	100	224
		93.71	237				234
		96.77	247				244
		98.90	257				254
		99.79	267				
		99.99	277				
		100	287				

Table 9. Results of hypsometric curve analyses for basins/watersheds 8–11.

Basin 8		Basin 9		Basin 10		Basin 11	
Area	Elevation	Area	Elevation	Area	Elevation	Area	Elevation
0.84	181	7.16	106	3.01	109	21.40	133
2.60	191	12.93	116	22.77	119	47.61	143
7.59	201	23.80	126	37.68	129	66.72	153
17.60	211	37.31	136	48.24	139	84.25	163
31.44	221	47.27	146	56.96	149	98.16	173
45.77	231	63.45	156	66.73	159	100	183
60.81	241	77.94	166	77.76	169		
74.85	251	84.42	176	85.91	179		
84.38	261	87.84	186	89.55	189		
92.42	271	91.63	196	93.25	199		
98.29	281	94.93	206	96.97	209		
99.80	291	97.06	216	99.18	219		
99.99	301	98.23	226	99.97	229		
		99.02	236	100	239		
		99.75	246				
		99.96	256				
		99.99	266				
		100	276				

The considered parameter such as Topographic Symmetry Factor (*T*) (Cox 1994) calculated for watersheds 9, 10 and 16 (Table 11) shows NNE to E lateral shifting of gully at watershed 10, and NW to WNW shift of gully segment at the western part of watershed 9. For watersheds other than 9, 10 and 16, parameters such as valley floor width to height ratio (*Vf*) and sinuosity index (*SI*) have been applied. Broad watersheds (9, 10 and 16) witnessed decipherable results than small gullies as the later are very dynamic and change their flow path during every monsoon or in alternate monsoons. It indicates low tectonic

Table 10. Results of hypsometric curve analyses for basins/watersheds 12–16.

Basin 12		Basin 13		Basin 14		Basin 15		Basin 16	
Area (%)	Elevation (m)	Area (%)	Elevation (m)	Area (%)	Elevation (m)	Area (%)	Elevation (m)	Area (%)	Elevation (m)
32.95	103	29.60	121	30.90	123	5.83	170	4.50	144
57.14	113	65.31	131	45.95	133	18.08	180	16.68	154
74.11	123	83.16	141	54.69	143	33.32	190	28.05	164
87.16	133	92.15	151	62.48	153	45.74	200	35.25	174
93.31	143	96.91	161	89.25	163	61.91	210	45.06	184
97.51	153	99.35	171	99.91	173	77.07	220	56.58	194
99.96	163	100	181	99.99	183	89.09	230	68.20	204
100	173					98.52	240	81.16	214
						99.97	250	92.54	224
						100	260	99.19	234
								99.95	244
								100	254

Table 11. Results of Transverse Topographic Symmetry Factor (T) from basins/watersheds 9, 10 and 16.

Basin 9			Basin 10			Basin 16		
<i>Da</i>	<i>Dd</i>	<i>T</i>	<i>Da</i>	<i>Dd</i>	<i>T</i>	<i>Da</i>	<i>Dd</i>	<i>T</i>
1.7	3.37	0.50	3.96	6.67	0.59	1.12	6.37	0.18
2.15	5.33	0.40	1.16	6.47	0.18	0.93	6.38	0.15
1.5	3.95	0.38	1.52	6.84	0.22	0.05	6.07	0.01
2.05	4.08	0.50	0.48	10.33	0.05	0.59	6.77	0.09
3.29	7.16	0.46	0.1	6.78	0.01	0.85	6.07	0.14
3.89	5.7	0.68	1.48	7.19	0.21	0.55	6.14	0.09
4.12	11.56	0.36	3.54	8.65	0.41	1.3	6.58	0.20
1.3	11.22	0.12	6.24	10.13	0.62	0.49	6.49	0.08
0.5	11.39	0.04						
3.05	12.95	0.24						
2.5	11.8	0.21						
0.08	9.2	0.01						
0.88	9.13	0.10						
0.78	9.98	0.08						
2.34	10	0.23						

control where the *Vf* magnitude is near 0 and a moderate tectonic control over the gully segments on the western part of the watersheds 9 and 10 (Table 11).

Normalized longitudinal profile analysis (Ayaz et al. 2018; Biswas and Paul 2021) performed for main gullies of the basins 9, 10 and 16 are fitted with linear and exponential regression curves (Table 12). A gully segment of watershed 10 shows significant variation in profile section (watershed 10b in Figure 7D). Comparing the regressions curves, it can be inferred that some structural elements intersect the gully at upstream and therefore give rise to depression in the profile. Such depression can also indicate rapid erosion and downstream deposition (Table 12).

The considered spot study as zones 1, 2 and 3 reveal local topographic expression with aligned faults/lineaments. Computation of channel *SI* determines the structural control on channel flow path. Figure 8A presents spatial-scale analyses in detail from these three zones.

Zone-1 incorporates an exposure in the area, which is easily understandable from the 3D representation (Figure 8B) with proper latitude/longitude and scale. The contour representation of the area is in Figure 8C. Figure 8B also includes the position of NNW-SSE directed Ramgarh fault and other lineaments. The major direction of physical slope face is the aspect map where most of the slope facets are northwest aligned (Figure 8D). The

Table 12. Linear and exponential regression analyses of normalized longitudinal profiles for the basins 9, 10 and 16.

Basins	Linear Regression ($y = mx + b$)	Exponential ($y = ae^{bx}$)
9a	$y = 0.4005x + 0.5995, R^2 = 0.9962$	$y = 0.6144e^{0.5054x}, R^2 = 0.9974$
9b	$y = -0.3892x + 0.9098, R^2 = 0.9678$	$y = 0.9247e^{-0.539x}, R^2 = 0.9881$
10a	$y = -0.2906x + 0.9287, R^2 = 0.8435$	$y = 0.9315e^{-0.359x}, R^2 = 0.8642$
10b	$y = -0.3562x + 0.9263, R^2 = 0.9441$	$y = 0.9361e^{0.467x}, R^2 = 0.9707$
16	$y = 0.2833x + 0.7148, R^2 = 0.9962$	$y = 0.7223e^{0.3317x}, R^2 = 0.995$

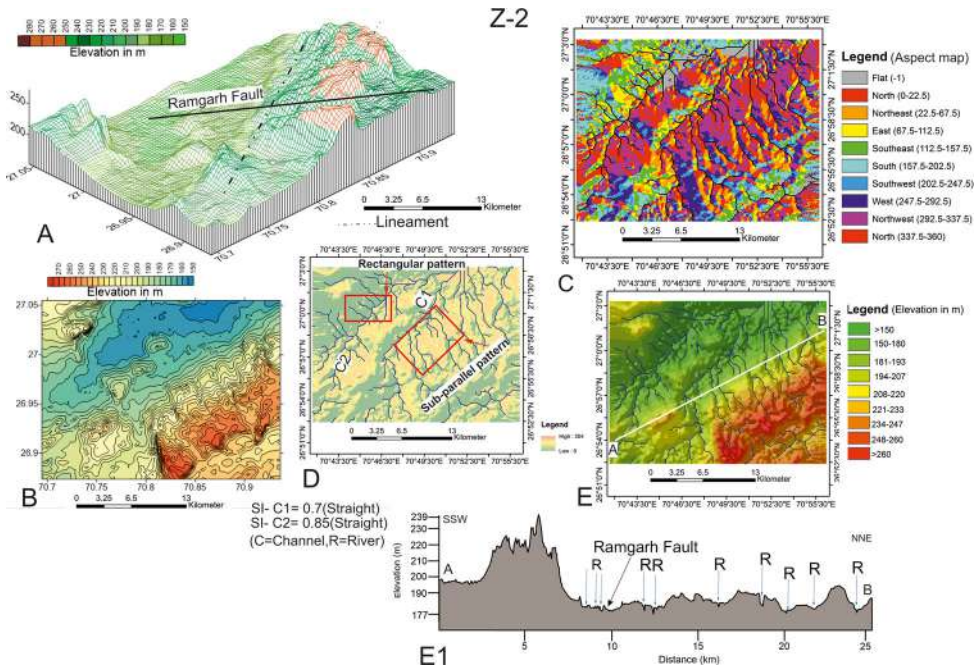


Figure 9. A. 3D representation of zone 2 with the overlapping of Ramgarh fault and lineament. B. Distinct identification of hilly patched with low elevated elongated valley identified and detail contour spacing with elevation. C. Slope aspect map of the area where most of the direction towards NW and N. D. Drainage orientation on hills shade map with distinct identification of rectangular and sub-parallel drainage pattern. E. Absolute relief map with intersecting drainage lines and alignment of AB line for elevation profile. E1. SSW-NNE AB section with fault/lineament and intersecting channels.

previous statement is also exemplified by Figure 8E and F, which shows most of the channels to be flowing towards NW. The major channels, C1 and C2 in Figure 8E, represent sub-parallel and rectangular drainage pattern, respectively. It denotes the tectonic interference. Position of Ramgarh fault confirms the structural control on drainage orientation. Rectangular pattern represents lineament/fault-guided nature of channels as the tributaries (Figure 8E). The trend of the rectangular channels also matches with the regional NNW-SSE and NE-SW trend. As per the calculated Sinuosity Index (SI) of channels, most channels come under the straight category, which indicate that the vertical incision and erosion is more than the lateral erosion. Elevation and depression from the sectional view (Figure 8F, F1) along the computed line AB supports the position of faults and channels in the area.

3D representation (Figure 9A) and contour representation (Figure 9B) of the area give an overall idea of the zone-2. The zone is characterized by a steep slope at the SE corner.

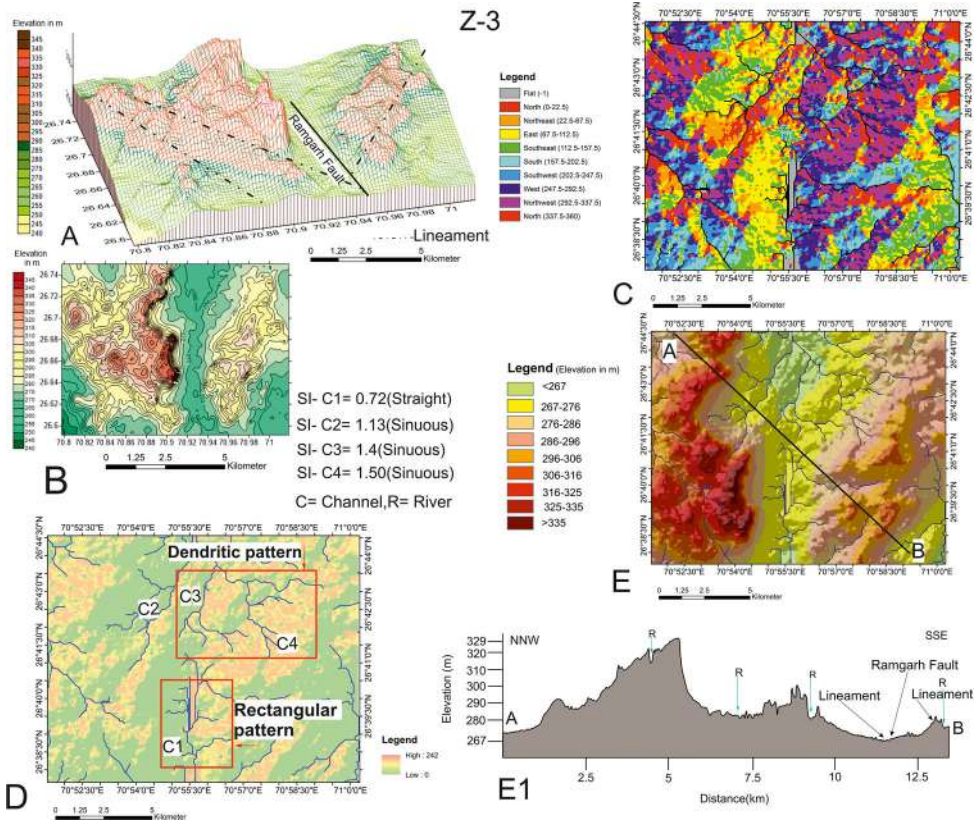


Figure 10. A.3D representation of zone 3 with the overlaying of Ramgarh Fault and lineaments. Elongated N-S hilly patches with two low elevated elongated valleys (N-S) identified B.Detail contour spacing of the area with elevation zones. C. Slope aspect map of the area where most of the slope direction towards E, W, NW and NE. D. Drainage orientation on hills shade map with distinct identification of dendritic and rectangular drainage pattern. Four channels are considered: C1-C4(C-Channel). E. Absolute relief map with intersecting drainage lines and alignment of AB line for elevation profile. E1.NNW-SSE AB section with Ramgarh Fault/lineaments and intersecting channels.

Ramgarh fault passes through the elevated zone related to the steep slope. Proper positions of this fault and other lineament are shown in Figure 9A. Major slope direction of the area is along northwest as per the aspect map (Figure 9C), which is also supported by the channels flow from northwestern direction (Figure 9D,E). Rectangular drainage pattern in the area represents the fault-controlled course of streams, whereas sub-parallel channels indicate that their paths are slope-controlled (Figure 9D). Calculated SI values of channels (1.0, 0.7) of the area indicate that they are straight. Thus, more vertical incision than the lateral erosion has worked on them. The sectional view along AB (Figure 9E) is shown in Figure 9E1, which gives better idea about the positions of channels, rivers and major faults.

The contour map (Figure 10B) of zone-3 represents a N-S trending valley like structure in between two ridges. Figure 10A supports this and shows that the valley is along the Ramgarh fault. Positions of other lineaments are also plotted in a 3 D representation (Figure 10A). Aspect map (Figure 10C) of the area shows the major slope directions, which are NW and SE. Arrangement of channels (Figures 10D,E) indicate the variation in slope directions of the area, obtained from the aspect map. Channel 2 (C2), Channel 3 (C3) and Channel 4 (C4) show dendritic drainage pattern, which can indicate gentle regional slopes or homogeneous

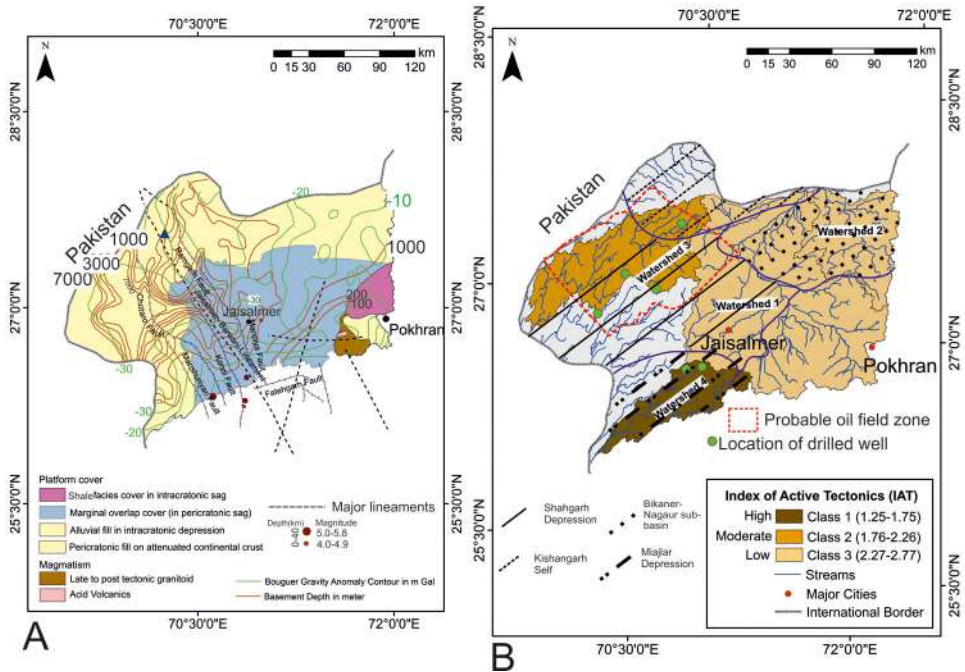


Figure 11. A. Detail of platform cover and magmatism of the Jaisalmer area with Bouguer anomaly. Earthquake epicenters marked with major fault lines and lineaments (modified from Narula et al. 2000). B. Map of watershed basis active tectonic zone with four tectonic sub-basins of Jaisalmer area. Probable oil fields are marked with six drilled wells to the basements (modified from <http://www.rajras.in/rajasthan/geography/minerals/hydrocarbon/> and Cozzi et al. 2012).

bedrock or fine grain sediment deposition. Channel 1 (C1) shows rectangular drainage pattern. This indicates major tectonic control of channels. Location of the Ramgarh fault supports the channel morphologic attributes (Figure E1).

5. Discussions

The spatial arrangement of drainage patterns connotes the structural signatures of the of the Jaisalmer shelf in with respect to of the regional slope and relief. Near the Manhera fault, channels flow westward and over the exposed Bhuana Formation, the flow path is restricted towards SW. It clearly denotes clearly that the elevated topography of the Kanoi fault acts as a water divide. Here, two watersheds originated. Hence, the SW streams are arranged in a parallel irregular layout without forming a watershed. Development of rectangular, trellis and complex barbed pattern signify fault lines over which the channels are oriented. The linear-scale analysis discloses the existing major fault lines along the master stream of each watershed where SL values have increased and channels are straight to sinuous. The results of the calculated ranges of IAT classify the watershed 1 as high, 3 as moderate, and 1 and 2 as low active. The classification is associated with existing faults, lineaments and spatial erosion rate that have restructured the shape of the watersheds.

Thus, the morphotectonic analysis of the Jaisalmer pericratonic basin gives a scope to determine the tectonic activeness of the basin. Analyses of the considered three spots also confirm the tectonic intervention in channel incision resulting straight flow

path of small gullies and inception of rectangular to sub-parallel drainage pattern. However, it is under the seismic zone III, i.e. moderate damage risk zone (Disaster Management & Relief and Civil Department, Rajasthan Government, 2021, Earthquake zones section; Earthquake hazard program 2021). As per the United States Geological Survey (USGS), major earthquakes in the study happened in the recent past with of 5.6 (on 08-Nov-1991) and 5.1 magnitudes (on 09-April-2009). According to Laul (2000), the NNW-SSE trending Kanoi fault is possibly related with seismicity. Earthquakes on 08-Nov-1991 and 20-Nov-1991 occurred due to reactivation of the Kanoi fault. Seismic studies disclose that the epicenters of the earthquakes fall on the Kanoi fault (Joshi et al. 1997). From the gravity map of Narula et al. (2000), it is well defined that the seismicity resulted from the emplacement of lower crustal or upper mantle materials at shallow depth.

The platform covers the area as fill, alluvial fill in intracratonic depression, marginal overlap of sag, and shell facies covering the intracratonic sag. The Bouguer anomaly contours and the basement depth indicate that both the lines are concentrated in the intracratonic depression area. It covers the marginal overlap of the sag region where most of the faults and lineaments are specified (Figure 11A). As per the morphotectonic study, the area falls under four watersheds (Figure 11B). Watersheds 1 and 2 are near-circular indicating a very low effect of active tectonics, whereas watersheds 3 and 4 are elongated and indicate moderate and high influence of active tectonics, respectively. The tectonically active watersheds belong to the Shahgarh and the Miajlar depressions. Channels of watershed 3 and 4 originated from the major NNW-SSE trending Ramgarh-Kanoi fault zone, which is an evidence of a strike-slip movement (Pandey et al. 2019b). It is sinistral in nature, as it is evident from NNE-SSW trending structural contours that extend towards NNW and then again turn NNE-SSW.

6. Conclusions

The study identifies few morphotectonic signatures of on the Jaisalmer rift basin and indirectly links them to sub-surface structures. The work can have a far-reaching implication in hydrocarbon exploration-related activities. The major outcomes are:

- The Jaisalmer basin consisting of several faults has been experiencing tectonic and seismic activities. The fault segments along the watersheds are tectonically active.
- The analysis of *IAT* with *SL*, *SI* and micro-scale hypsometric analysis reflect that the Jaisalmer basin is tectonically active.
- The three individual morphotectonic spot studies reveal the imprint of existing faults and lineaments. It points out the role of active tectonics on small gullies in micro-scale. The Shahgarh depression and the Miajlar depression, along with Kishangarh shelf are mostly under tectonically active watersheds.
- Hydrocarbon fields are located in the Shahgarh depression and the Miajlar depression area, which belong to tectonically active watersheds – 3 and 4.
- There is no direct relation between morphotectonic analysis with hydrocarbon exploration and development. However, such studies help to assess the tectonic sensitivity of the basin and thus pinpoints areas where the sub-surface faults need to be relooked in terms of reactivation. The sub-surface fluid flow pathways will also be impacted in the tectonically active zones of the basin.

Acknowledgements

Seed project (*grant number RD/0120-PSUCE19-001*) received from Center of Excellence in Oil, Gas and Energy, IIT Bombay during February to August 2021 awarded to SM is acknowledged. Thanks to S. N. Karnekar and J. Shrikanth for helping SM in project-related paper works. We thank Chief Editor, Associate Editor, anonymous Reviewers and the proofreading team.

Disclosure statement

No potential conflict of interest was reported by the authors.

All funding agencies acknowledged in Acknowledgements section.

All authors have seen and have approved submission.

Author credit statement

MB:Analyses, draft writing

MPG, SS, BM:Analyses and partial draft writing,

SM, SDG:Supervision, partial writing and finalization of draft

ORCID

Thota Sivasankar  <http://orcid.org/0000-0003-2422-8731>

References

- Ahmad A, Aquil M. 2000. Microfacies analysis of Kuldhara limestone, Jaisalmer formation (Cretaceous-oxfordian), Western Rajasthan, India. *Eur. J. Geol.* 12(1):75–88.
- Ahmad A, Upadhyay G, Noufal KN. 2013. Petrography and diagenetic history of the Jajiya member sediments, Jaisalmer formation (Middle to Late Jurassic), Western India. *Proc Indian Acad Sci* 115(4):895–901.
- Ahmad F, Amir M, Quasim M, Absar N, Ahmad AH., 2022. Petrography and geochemistry of the Middle Jurassic Fort Member Sandstone, Jaisalmer Formation, Western India: Implications for weathering, provenance, and tectonic setting. *Geol J.* doi:10.1002/gj.4372.
- Alam MM. 1993. Sandstone Diagenesis and Petrofacies of Jaisalmer Formation (Middle Jurassic) Western Rajasthan, India, India: Unpublished M. Phil. dissertation, Aligarh Muslim University, Aligarh. p. 136.
- Alberti M, Pandey DK, Sharma JK, Swami NK, Uchman A. 2017. Slumping in the upper Jurassic Baisakhi formation of the Jaisalmer Basin, western India: Sign of synsedimentary tectonics? *J Palaeogeograph.* 6(4):321–332.
- ALOS World 3D-30 m (AW3D30). n.d. The ALOS global digital surface model (AW3D30) by Japan Aerospace Exploration Agency: The Japan Aerospace Exploration Agency (JAXA). <https://www.eorc.jaxa.jp/ALOS/en/index.htm>.
- Anand AK, Pradhan SP. 2019. Assessment of active tectonics from geomorphic indices and morphometric parameters in part of Ganga basin. *J Mt Sci.* 16(8):1943–1961.
- Andreani L, Klaus P, Stanek Gloaguen R, Krentz O, Domínguez-González L. 2014. DEM-based analysis of interactions between tectonics and landscapes in the ore mountains and Eger Rift (East Germany and NW Czech Republic). *Remote Sens.* 6(9):7971–8001.
- Ansa V, Mangold N. 2006. New observations of Warrego Valles, Mars: evidence for precipitation, and surface runoff. *Planet Space Sci.* 54(3):219–242.
- Asher R, Shing SD, Whiso K, Kapoor PN. 2021. Cretaceous-Paleogene dinoflagellate cyst and foraminiferal events in the subsurface sedimentary successions of Jaisalmer Basin, India: insights from a newly drilled well in the area. In: Shridhar KN, editor. *ONGC Bulletin*; Vol. 56., No. 1., p 123–134., ISSN 0537-0094.
- Awasthi AM. 2002. Geophysical exploration in Jaisalmer Basin – A case history. *Geohorizons.* 1–6.
- Ayaz S, Biswas M, Dhali K. 2018. Morphotectonic analysis of alluvial fan dynamics: comparative study in spatio-temporal scale of Himalayan foothill, India. *Arab J Geosci.* 11(2):1–16.

- Bafna PC, Dhaka BS. 1999. Industrial grade limestone deposits of Tertiary period in Western Rajasthan. In Paliwal, BS, editors. Geological evolution of Northwestern India, Scientific Publishers (India), Jodhpur. p. 210–215. ISBN. 81-7233-210-6
- Bhadu B, Mondal, A. 2018. Facies analysis and reservoir characterization of mesozoic-cenozoic sediments from drilled well section at Bankia structure, Jaisalmer Basin. ONGC Bull. 53(1):106.
- Bhandari A. 2008. Ostracode biostratigraphy and carbon and oxygen isotopic studies across the Paleocene/Eocene boundary in the subsurface of Jaisalmer Basin, Rajasthan, India. *Senckenberg Lethaea*. 88(1):67–76.
- Biswas M, Dhara P. 2019. Correction to: Evolutionary characteristics of meander cut-off – A hydro-morphological study of the Jalangi River, West Bengal. *India Arab J Geosci*. 12:739.
- Biswas M, Paul A. 2021. Application of geomorphic indices to Address the foreland Himalayan tectonics and landform deformation– Matiali-Chalsa– Baradighi recess, West Bengal, India. *Quater Int*. 585: 3–14. DOI.
- Biswas M, Puniya MK, Gogoi MP, Dasgupta S, Mukherjee S, Kar NR. 2022. Morphotectonic analysis of petroliferous Barmer rift basin (Rajasthan, India). *J Earth Syst Sci*. (In press).
- Bonde SD. 2010. A new genus of podocarpaceous wood from the Lathi Formation (Early Jurassic) of Rajasthan, India. *Geophytology*. 38:19–24.
- Brice JC. 1964. Channel patterns and terraces of the Loup river in Nebraska. Geological Survey Professional Paper 422-D. Washington, D2–D41.
- Bull WB, McFadden LD. 1977. Tectonic geomorphology north and south of the Garlock fault, California. *Geomorphology in Arid Regions*. Proceedings of the Eight Annual Geomorphology Symposium (Ed. DO Doehring). Binghamton, NY: State University of New York at Binghamton. p. 115–138.
- Chidambaram L. 1991. Mesozoic biostratigraphy, paleo-bathymetry and paleobiogeography of subsurface sediments in western Rajasthan. In: Pandey J, Banerjee V, editors. Proceedings of the conference on integrated exploration research: Achievements and perspectives. Shiva Offset Press, Dehradun; p. 179–187.
- Cox RT. 1994. Analysis of drainage-basin symmetry as a rapid technique to identify areas of possible quaternary tilt-block tectonics: an example from the Mississippi Embayment. *Geol Soc Am Bull*. 106(5): 571–581.
- Cozzi A, Rea G, Craig J. 2012. From global geology to hydrocarbon exploration: Ediacaran-Early Cambrian petroleum plays of India, Pakistan and Oman. In: Bhat GM, Craig J, Thurow JW, Thusu B, Cozzi A, editors. *Geology and hydrocarbon potential of neoproterozoic–Cambrian basins in Asia*. *Geol Soc London Special Publ*. 366(1):131–162.
- Czerniawska J, Chlachula J. 2018. Report. Field trip in the Thar desert. *Landform Anal*. 35:21–26.
- Das Gupta SK. 1975. A revision of Mesozoic-Tertiary stratigraphy of the Jaisalmer Basin, Rajasthan. *Indian J Earth Sci*. 2:77–94.
- Dasgupta S, Biswas M, Mukherjee S, Chatterjee R. 2022. Structural evolution and sediment depositional system along the transform margin-Palar–Pennar basin, Indian east coast. *J Petrol Sci Eng*. 211:110155.
- Dasgupta S, Mukherjee S. 2017. Brittle shear tectonics in a narrow continental rift: asymmetric non-volcanic Barmer basin (Rajasthan, India). *J Geol*. 125(5):561–591.
- Dasgupta S, Mukherjee S. 2019. Remote sensing in lineament identification: examples from Western India. In Andrea B, Åke F, editors. *Developments in Structural Geology and Tectonics*. Vol. 5. Elsevier; p. 205–221, ISSN 2542-9000, ISBN 9780128140482.
- Dehbozorgi M, Pourkermani M, Arian M, Matkan AA, Motamedi H, Hosseiniasl A. 2010. Quantitative analysis of relative tectonic activity in the Sarvestan area, central Zagros, Iran. *Geomorphology*. 121(3-4):329–341.
- Disaster Management, Relief & Civil Defense Department. 2021, July, 29. Earthquake Zones. Government of Rajasthan. <http://www.dmrelief.rajasthan.gov.in/index.php/citizen-charter/maps-ofrajasthan/earthquake-zones>
- Drummond SA, Erkeling G. 2014. Drainage pattern. *Encyclopedia of Planetary Landforms*. New York: Springer Science Business Media. doi:10.1007/978-1-4614-9213-9_119-1.
- EarthExplorer (EE). n.d. United States Geological Survey (USGS). <https://earthexplorer.usgs.gov/>.
- Earthquake Hazards Program. 2021. Search earthquake catalog, July 2. USGS (United States. Geological Survey) website: <https://earthquake.usgs.gov/earthquakes/search/>.
- Flugel JT, Eckardt DF, Cotterill P. 2015. The present day drainage patterns of the Congo River System and their Neogene evolution. In: de Wit MJ, editor. *Geology and resource potential of the Congo basin, regional geology reviews*. Berlin Heidelberg: Springer; p. 315–337. doi:10.1007/978-3-642-29482-2_15.

- Hack J. 1957. Studies of Longitudinal Stream Profiles in Virginia and Maryland. Geol Survey Profession Paper. 294B:45–95.
- Hamdouni RE, Irigaray C, Fernández T, Chacón J, Keller EA. 2008. Assessment of relative active tectonics, southwest border of the Sierra Nevada (southern Spain). *Geomorphology*. 96(1-2):150–173.
- Hare PW, Gardner TW. 1985. Geomorphic Indicators of Vertical Neotectonism along Converging Plate Margins, Nicoya Peninsula, Costa Rica. In: Morisawa M, and Hack JT, editors, *Tectonic geomorphology. Proceedings of the 15th Annual Binghamton Geomorphology Symposium*, Allen and Unwin, Boston, p. 123–134.
- Horacio J. 2014. River Sinuosity Index: Geomorphological characterisation. CIREF and Wetlands International European Association. Santiago de compostela University; p. 8.
- Horton RE. 1945. Erosional development of streams and their drainage basins: hydrophysical approach to quantitative morphology. *Geol Soc Am Bull*. 56(3):275–370.2.0.CO;2].
- Joshi DD, Dharman R, Saxena AK. 1997. Jaisalmer earthquake of 1991; Its effects and tectonic implications. *J Geol Soc India*. 49:433–436.
- Kachhara RP, Jodhawat RL. 1999. Bivalve biostratigraphy of the Jaisalmer Formation, Western Rajasthan, India. In: Paliwal BS, editor. *Geological evolution of Northwestern India*, Scientific Publishers (India), Jodhpur; p. 109–117. ISBN. 81-7233-210-
- Kale VS, Sengupta S, Achyuthan H, Jaiswal KM. 2014. Tectonic controls upon Kaveri River drainage, cratonic Peninsular India: Inferences from longitudinal profiles, morphotectonic indices, hanging valleys and fluvial records. *Geomorphol*. 227:153–165.
- Kalia P, Kintso R. 2006. Planktonic foraminifera at the Paleocene/Eocene boundary in the Jaisalmer Basin, Rajasthan, India. *Micropaleontology*. 52(6):521–536.
- Kalita, K.D. 2015. New report of isocrinid crinoid *Chariocrinus* from the Jurassic of Jaisalmer, Rajasthan, India. *J Geol Soc India*. 86(5):597–604.
- Kar A. 2011. Quaternary geomorphic processes and landform development in the Thar Desert of Rajasthan. In: Bandyopadhyay S, editor. *Landforms processes & environment management*. Kolkata (India): ACB publication; p. 223–254. ISBN 81-87500-58-1 2011.
- Kaur G, Kaur P, Ahuja A, Singh A, Saini J, Agarwal P, Bhargava ON, Pandit M, Goswami RG, Acharya K, et al. 2020. Jaisalmer golden limestone: a heritage stone resource from the desert of Western India. *Geoheritage*. 12(3):1–16.
- Keller EA, Pinter N. 2002. *Active tectonics: Earthquakes, uplift, and landscape*. 2nd ed. Englewood Cliffs (NJ): Prentice Hall, p. 362.
- Krishna Brahman N. 1993. Gravity and seismicity of Jaisalmer region, Rajasthan. *Current Science*. 64: 837–840.
- Lal M. 1994. Biosedimentological Studies of cores from Cambay, Krishna-Godavari and Rajasthan Basins. In: Biwas SK, Pandey J, Dave A, Maithani A, Garg P, Thomas NJ, editors. *Proceeding of the Second Seminar on Proliferous Basins of India*. Vol 3: Himalayan Foothills, Vindhyan and Gondwana Basins, Geoscientific Studies and hydrocarbon Exploration Techniques. Dehradun: Indian Petroleum Publishers; p. 185–200. ISBN 81-900361-0-6.
- Laul V. 2000. Kanoi fault and its possible relation to Jaisalmer earthquakes. *J Geol Soc India*. 55:681–681.
- Lee C, Tsai LL. 2010. A quantitative analysis for geomorphic indices of longitudinal river profile: A case study of the Choushui River, Central Taiwan. *Environ Earth Sci*. Springer Verlag. 59(7):1549–1558.
- Liu F, Peng Y, Zhang W, Pedrycz W. 2017. On consistency in AHP and fuzzy AHP. *J Syst Sci Inform*. 5(2):128–147.,
- Mahender K, Banerji RK. 1990. Petrography, diagenesis and depositional environments of Middle Jurassic Jaisalmer Carbonates, Rajasthan, India. *Indian J Earth Sci*. 17:194–207.
- Mahmood S, Gloaguen R. 2012. Appraisal of active tectonics in Hindu Kush: Insights from DEM derived geomorphic indices and drainage analysis. *Geosci Front*. 3(4):407–428.
- Mandal S, Sarkar S. 2016. Overprint of neotectonism along the course of River Chel, North Bengal, India. *J Paleogeograph*. 5(3):221–240.
- Miall AD. 1977. A review of the braided river depositional environment. *Earth Sci Rev*. 13(1):1–62.
- Mitra P, Mukherjee MK, Mathur BK, Bhandari SK, Qureshi SK, Bahukhandi GC. 1993. Exploration and hydrocarbon prospect in Jaisalmer Basin, Rajasthan. In: Biwas SK, Pandey J, Dave A, Maithani A, Garg P, Thomas NJ, editors. *Proceeding of the Second Seminar on Proliferous Basins of India*. Vol 2: West Coast Basins. Indian Petroleum Publishers. Dehradun; p. 235–284. ISBN 81-900361-0-6.
- Morisawa M. 1985. *Rivers*. Longman. (no. of pages: 222. Price: £12.95). ISBN 0-582-48982-2.
- Moussi A, Rebaï N, Chaieb A, Saâdi A. 2018. GIS-based analysis of the Stream Length-Gradient Index for evaluating effects of active tectonics: a case study of Enfidha (North-East of Tunisia). *Arab J Geosci*. 11(6):123.

- Mude SN, Jagtap SA, Kundal P, Sarkar PK, Kundal MP. 2012. Paleoenvironmental significance of ichnofossils from the Mesozoic Jaisalmer Basin, Rajasthan, North Western India. *Proceedings of the International Academy of Ecology and Environmental Sciences* 2, p. 150–167.
- Narula PL, Acharyya SK, Banerjee J. 2000. *Seismotectonic Atlas of India and its Environs*. Geological Survey of India. New Delhi. ISSN: 02540436.
- Nigam AN, Tripathi RP, Singh HS, Gambhir RS, Lukose NG. 1989. Mossbauer studies on Ghotaru Well No. 1 of the Jaisalmer Basin. *Fuel*. 68(2):209–212.
- Pandey DK, Chowdhury S. 2010. Sedimentary cycles in the Callovian-Oxfordian of the Jaisalmer Basin, Rajasthan, western India. *Volumina Jurassica VIII*: p. 131–162.
- Pandey DK, S, Bahadur, T.E.J C, Swami N, Poonia D, Jingeng S. 2012. A review of the lower–lowermost Upper Jurassic facies and stratigraphy of the Jaisalmer Basin, western Rajasthan, India. *Volumina Jurassica*. 10:61–82.
- Pandey DK, Sha J, Choudhary S. 2006. Depositional history of the early part of the Jurassic succession on the Rajasthan Shelf, western India. *Prog Nat Sci*. 16:176–185.
- Pandey R, Kumar D, Maurya AS, Pandey P. 2019a. Evolution of gas bearing structures in Jaisalmer Basin (Rajasthan) India. *J Indian Geophys Union*. 23:398–407.
- Pandey R, Kumar D, Maurya AS, Pandey P. 2019b. Hydrocarbon generation potential of source rocks in Jaisalmer Basin, Rajasthan, India. *Curr Sci*. 116(5):822–827.
- Pandey R, Maurya AS. 2020. Hydrocarbon Uncertainty Based on Facies Analysis: Middle Jurassic Sequence (Jaisalmer Formation), Jaisalmer Basin, Rajasthan. *J Geol Soc India*. 95(3):301–307.
- Pandey R, Nonia BP, Mahanti S, Pradhan UC, Maurya AS. 2019c. Geocellular Model for Tertiary Reservoirs in Manhera Tibba Gas Field, Jaisalmer Basin, Rajasthan, India. 2018 International Conference and Exhibition, Cape Town, South Africa. Search and Discovery Article #20456.
- Pareta K, Pareta U. 2011. Quantitative morphometric analysis of a watershed of Yamuna basin, India using ASTER (DEM) data and GIS. *Int J Geomatic Geosci*. 2:248–269.
- Pati JK, Malviya VP, Prakash K. 2006. Basement re-activation and its relation to Neotectonic activity in and around Allahabad, Ganga Plain. *J Indian Soc Remote Sens*. 34(1):47–56.
- Patra A, Shukla DA. 2020. Geochemical signatures of Late Paleocene sandstones from the Sanu Formation, Jaisalmer basin, western India. Implication for Provenance, Weathering and Tectonic Setting. *J Earth Syst Sci*. 129:81.
- Patra A, Singh BP. 2015. Facies characteristics and depositional environments of the Paleocene–Eocene strata of the Jaisalmer basin, western India. *Carbonate Evap*. 30(3):331–346.
- Paul A, Biswas M. 2019. Changes in river bed terrain and its impact on flood propagation – a case study of River Jayanti, West Bengal, India. *Geom Nat Hazards Risk*. 10(1):1928–1947.
- Prakash K, Mohanty T, Pati JK, Singh S, Chaubey K. 2017. Morphotectonics of the Jamini River basin, Bundelkhand Craton, Central India; using remote sensing and GIS technique. *Appl Water Sci*. 7(7): 3767–3782.,
- Rai J, Garg R. 2007. Early callovian nannofossils from the Kuldhar section, Jaisalmer, Rajasthan. *Curr Sci*. 92:816–820.
- Rai PK, Mohan K, Mishra S, Ahmad A, Mishra VN. 2017. A GIS-based approach in drainage morphometric analysis of Kanhar River Basin, India. *Appl Water Sci*. 7(1):217–232.,
- Ramírez-Herrera MT. 1998. Geomorphic assessment of active tectonics in the Acambay Graben, Mexican volcanic belt. *Earth Surf Process Landform*. 23(4):317–332.
- Roy AB, Jakhar SR. 2002. *Geology of Rajasthan (Northwest India, Precambrian to recent)*, Scientific Publishers (India), Jodhpur. ISBN: p. 9788172339722.
- Saha S, Das SS, Mondal S. 2021. Gastropod biozonation for the Jurassic sediments of Kutch and Jaisalmer Basins and its application in Interbasinal Correlation. In: Banerjee S, Sarkar S, editors. *Mesozoic stratigraphy of India: A multi-proxi approach*. Cham: Springer; p. 333–372. ISBN 978-3-030-71370-6.
- Sajadian M, Pourkermani M, QorasHi M, Moghadda NH. 2015. The analysis of transverse topographic symmetry factor (T Index) in the Chekene-Mazavand, North East Iran. *OJG*. 05(11):809–820.
- Satty TL. 1980. *The analytical hierarchy process: Planning, priority setting, resource allocation*, New York: McGraw-Hill International Book Company. ISBN: 0070543712, 9780070543713.
- Schumm SA, Khan HR. 1972. Experimental study of channel patterns. *Geol Soc Am Bull*. 83:1 755–70.
- Schumm SA. 1956. The evolution of drainage systems and slopes in bad lands at Perth, Amboi, New Jersey. *Geol Soc Am Bull*. 67(5):597–646.2.0.CO;2]
- Sharma JK, Pandey DK. 2016. Taxonomy of late Bathonian–Oxfordian ammonites from the Jaisalmer Basin: Implications for intrabasinal litho- and biostratigraphic correlations. *J Palaeontol Soc India*. 61(2):249–266.

- Sigal J, Singh NP, Lys M. 1971. Paleocene-Eocene boundary in the Jaisalmer area, India. *J Foraminifer Res.* 1(4):190–194.
- Singh CK, Venkatesh HS, Gopinath G, Pichamuthu DV, Sawkar RH, Krishnamurthy P. 2015. Middle Ganga plain; may be on the verge of seismic shock. *J Geol Soc India.* 85(4):511–513.
- Singh L. 2000, as referred in West Rajasthan Basin. *Oil and Gas fields of India.* Indian Petroleum Publishers Dehradun. ISBN: 81-900361-9-x
- Singh NP, Sharma M, Jha N, Tewari R, Saleem M, Matsumaru K, Ehiro M, Kojima S, Jauhri AK, Misra PK, et al. 2006. Mesozoic lithostratigraphy of the Jaisalmer basin, Rajasthan. *J Palaeontol Soc India.* 51: 1–25.
- Singh NP. 1996. Mesozoic-tertiary biostratigraphy and biochronological datum planes in Jaisalmer Basin, Rajasthan. In Pandey J, Azmi RJ, Bhandari A, Dave A, editors. XV Indian Colloquium on Micropaleontology and Stratigraphy. Dehradun (India); p. 63–89.
- Singh NP. 2007. Cenozoic litho-stratigraphy of the Jaisalmer Basin, Rajasthan. *J Paleontol Soc India.* 52(2):129–154.
- Sinha AK, Yadav RK, Qureshi SM. 1993. Status of exploration in south Shahgarh Sub-basin of Jaisalmer Basin, Rajasthan. In: Biwas SK, Pandey J, Dave A, Maithani A, Garg P, Thomas NJ, editors. *Proceeding of the Second Seminar on Proliferous Basins of India. Vol 2: West Coast Basins.* Indian Petroleum Publishers. Dehradun. p. 285–333. ISBN 81-900361-0-6.
- Smith JS, Chandler J, Rose J. 2009. High spatial resolution data acquisition for the geosciences: kite aerial photography. *Earth Surf Process Landform.* 34(1):155–161.
- Srivastava S, Pandey VJ. 1996. Biofacies variation in subsurface sequence of Lunar-Miajlar area. Jaisalmer Basin, Rajasthan. In Pandey J, Azmi RJ, Bhandari A, Dave A, editors. XV Indian colloquium on micropaleontology and stratigraphy. Dehradun (India); p. 55–61.
- Srivastava SK. 1966. Jurassic microflora from Rajasthan, India. *Micropaleontology.* 12(1):87–103.
- Strahler AN. 1952. Hypsometric (area-altitude) analysis of erosional topography. *Geol Soc Am Bull.* 63(11):1117–1142.2.0.CO;2]
- Strahler AN. 1957. Quantitative analysis of watershed geomorphology. *Trans AGU.* 38(6):913–920.
- Sudan CS, Sahni AK, Sharma UK. 2000. Trace fossils from the Jurassic sequence of Jaisalmer basin, Rajasthan. *J Palaeontol Soc India.* 45:165–171.
- Surabhi KN, Biswas M, Mukherjee S. Submitted. Morpho-tectonic investigation of petroliferous Cambay rift basin (Gujarat, western India). *J Indian Soc Rem Sens* (under Review).
- Takieh E, Ghorashi M, Rezaie F. 2015. The transverse topographic symmetry Factor of Darakeh stream in the North Tehran, Iran. *OJG.* 05(11):770–779.
- Torsvik TH, Pandit MK, Redfield TF, Ashwal LD, Webb SJ. 2005. Remagnetization of Mesozoic limestones from the Jaisalmer basin, NW India. *Geophys J Int.* 161(1):57–64.
- Upadhyay H. 1991. Depositional Environments and reservoir characteristics of Jaisalmer Formation, Jaisalmer Basin, Rajasthan. In: Pandey J, Banerjee V, editors. *Proceedings of the Conference on Integrated Exploration Research: Achievements and Perspectives.* Shiva Offset Press, Dehradun; p. 349–363.
- Verma D, Jadhav GN, Biswal TK, Jena SK, Sharma N. 2012. Characterization of hydrocarbon-bearing fluid inclusion in sandstones of Jaisalmer Basin, Rajasthan: A preliminary approach. *J Geol Soc India.* 80(4):505–514.
- Whipple K, Wobus C, Crosby B, Kirby E, Sheenan D. 2007. New tools for quantitative geomorphology: Extracting and interpretation of stream profiles from digital topographic data. *GSA Annual Meeting, Boulder, CO.*
- Wobus C, Whipple K, Kirby E, Snyder N, Johnson J, Spyropoulou K, Crosby B, Sheehan D. 2006. Tectonics from topography: procedures, promise, and pitfalls. In Willet SD, Hovius N, Brandon MT, Fisher DM, editors. *Tectonics, climate, and landscape evolution.* Geo Soc America, United States; 398, p. 55–74.
- Zadan K, Arbab AK. 2015. A review on Lithostratigraphy and Biostratigraphy of Jaisalmer basin, western Rajasthan, India. *Int Res J Earth Sci.* 3:37–45. ISSN 2321–2527.
- Zavoianu I. 1985. *Morphometry of drainage basins (developments in water science 20).* Vol. 2. Elsevier.
- Zutshi PL, Panwar MS. 1997. *Geology of petroliferous basins of India, Rajasthan section.* Dehradun, India: KDM Institute of Petroleum Exploration: Oil & Natural Gas Corporation Ltd.; p. 63–69.

Appendix

Name of the Dataset: C1_DEM_16b_2005-2014_V3R1_73E24N_G43T, Theme: Terrain, Keywords: Cartosat-1, DEM, Stereo data, India, ISRO, NRSC, Use Constraints: As per NRSC Data Dissemination Policy, Purpose of creating data: Seamless DEM from IRS data, Spheroid/Datum: GCS, WGS-1984, Name of the Satellite: Cartosat-1, Sensor : PAN(2.5m), Stereo Data.

Vector file for administrative boundary of the study area was downloaded from the ArcGIS Hub (URL: <https://hub.arcgis.com>; accessed on 17-Jan-2020).

Landsat OLI 8 data of the study area was collected from USGS (United States Geological Survey) – EarthExplorer (EE) n.d. (URL: <https://earthexplorer.usgs.gov>; accessed on 21-Feb-2020).

ALOS (Advanced Land Observing Satellite) Global Digital Surface Model ‘ALOS World 3D-30 m (AW3D30) n.d.’ was collected from the Earth Observation Research Center of Japan Aerospace Exploration Agency (<https://www.eorc.jaxa.jp/ALOS/en/aw3d30/index.htm>, accessed on 03-April-2020)

Sentinet-2 MSI Level-2A data was collected from Copernicus, European Space Agency (ESA), European Union (<https://earthengine.google.com>, accessed on 28-01-2021)

GIS software viz. QGIS (ver.3.12, year 2020) and Global Mapper (ver. 2019) were used for performing DEM and raster-based analyses. Vector layers of drainage and lineaments have been extracted using digitiser tools. Inbuilt raster tools are used to perform analyses of profiles, ridges/lineaments, drainage and hypsometric curve.

Spreadsheet software (a part of Excel Office, ver. 2021) was used to perform statistical calculations e.g. linear, exponential, logarithmic and power regression.